Scientific Research Publishing

Journal of Power and Energy Engineering, 2026, 14(3), 53-83
https://www.scirp.org/journal/jpee
ISSN Online: 2327-5901
ISSN Print: 2327-588X

Two-Stage Virtual Power Plant Bi-Level Hybrid Game Model Considering Photovoltaic Uncertainty under Blockchain Technology

Jiahang Xu[1*], Junxiang Li[1,2], Yulu Li[1]

[1]Business School, University of Shanghai for Science and Technology, Shanghai, China
[2]School of Intelligent Emergency Management, University of Shanghai for Science and Technology, Shanghai, China
Email: *xujiahangsiomonxu1@163.com

How to cite this paper: Xu, J.H., Li, J.X. and Li, Y.L. (2026) Two-Stage Virtual Power Plant Bi-Level Hybrid Game Model Considering Photovoltaic Uncertainty under Blockchain Technology. *Journal of Power and Energy Engineering*, **14**, 53-83.
https://doi.org/10.4236/jpee.2026.143003

Received: February 28, 2026
Accepted: March 16, 2026
Published: March 19, 2026

Abstract

With the opening of the electricity retail market and the surge in the number of prosumers, distributed energy trading is playing an increasingly prominent role in the electricity market. To address the challenges posed by photovoltaic (PV) output uncertainty and to optimize resource allocation while reducing energy waste, this paper proposes a two-stage bi-level hybrid game model based on blockchain technology. In the first stage, leveraging blockchain technology, the microgrid operator (MGO) monitors the production and consumption of the prosumer cluster and establishes revenue models for both entities. The distributionally robust optimization (DRO) method based on the Wasserstein distance is employed to handle the uncertainty of PV output. Subsequently, the MGO and the shared energy storage operator (SESO) form a virtual power plant (VPP) alliance to enhance overall benefits and optimize system electricity consumption behavior, and based on the blockchain trading platform, a Stackelberg game is conducted between the upper-level alliance and the lower-level prosumer cluster to determine trading and dispatch strategies. In the second stage, internal benefits within the alliance are distributed via Nash bargaining. Numerical simulation results ultimately demonstrate that the proposed model can effectively maximize the benefits for all three parties and optimize system energy dispatch, verifying its correctness and effectiveness.

Keywords

Blockchain, Hybrid Game, Distributionally Robust Optimization, Virtual Power Plant, Photovoltaic Prosumer, Nash Negotiation

1. Introduction

1.1. Motivation

Under the "dual-carbon" goal of "striving to achieve carbon peaking by 2030 and carbon neutrality by 2060" [1], the trading of renewable energy sources such as wind and light will bring unlimited opportunities for the development of new electricity markets. Although renewable energy is abundant, its intermittency and volatility bring new challenges for its management methods and scheduling strategies [2] [3]. VPP, through advanced technology platforms and developed network systems, aggregates thousands of distributed and uncontrollable renewable energy units for efficient development and utilization [4].

1.2. Literature Overview

Shared energy storage (SES) works with single or multiple independent storage stations and provides flexible energy storage services to users in the form of leasing and charging/discharging services with the characteristics of "cloud services" [5]. Existing literature and studies have demonstrated that the inclusion of SES in VPP not only enhances the revenue and environmental benefits for both parties but also optimizes the energy scheduling of the system as well as the energy use strategy. Wang W *et al.* [6] proposed a two-layer decision model, which is used for solving the problem of shared energy storage configuration and optimization of multi-VPP system operation.

Lin M *et al.* [7] optimize the energy scheduling and allocation of the DSO-VPP system, a Stackelberg cooperative hybrid game framework is proposed. Pan Y *et al.* [8] proposed a shared hybrid energy storage operation optimization and cost allocation strategy for microgrid groups considering flexible ramping capability.

Due to the high uncertainty of distributed energy output, both the economic efficiency and system operational effectiveness can incur certain losses for all parties involved in electricity trading and scheduling. In practice, the operation of the system will be affected by the uncertainty of the distributed energy output. Wasserstein distance, as a mathematical model describing the "distance" between the uncertainty and the actual quantity [9], provides an important theoretical support for the construction of DRO model, which provides a more stable and risk-resistant capability for the system. Li W *et al.* [10] used fuzzy sets based on the Wasserstein distance to determine the prediction error of wind and PV outputs to create a two-layer optimization model for coordinating DR bidding decisions internally and externally at the VPP. Liu H *et al.* [11] proposed a piecewise affine formulation combining VPP profit and CVaR to hedge the market price risk; then, a data-driven distributed robust mode optimization model is constructed using Wasserstein fuzzy sets due to the uncertainty in the market price and wind prediction errors.

The trading and scheduling of energy between VPP, shared energy storage operator (SESO), and groups of prosumers are often connected through a hybrid gaming approach [12]. The methods used to solve the Stackelberg game model are

mature in the existing research, but the distribution of benefits in the cooperative game needs to be selected according to the different characteristics of the participants, such as the Nash bargaining method and the Shapley value method. Chang W *et al.* [13] proposed a day-ahead bidding strategy to target risk aversion in the wholesale electricity market, and the conditional value-at-risk is used as a risk criterion to quantify and hedge risks in the market and to categorize real-time electricity price situations. Electricity trading behavior within a virtual power plant is then described through Stackelberg game theory. Shang Y *et al.* [14] proposed a ladder Shapley value allocation method as a means of achieving a reasonable profit distribution based on the capacity of the market prior to the day of participation. Li N *et al.* [15] proposed a real-time pricing (RTP) framework that integrates stochastic unit commitment (UC) and carbon-aware generation scheduling within a multi-energy generation system, while incorporating an uncertain demand response (DR) program to incentivize user participation, and uses the Stackelberg game to realize electricity pricing. Gao Y *et al.* [16] designed a real-time pricing (RTP) mechanism for the smart grid that integrates multiple supply-side generating units with distributed renewables and energy storage on the demand side, where the strategic interactions are captured in a Stackelberg game framework. Dai Y *et al.* [17] proposed and analyzed a real-time pricing scheme for a smart grid with multiple retailers and residential users, where a Stackelberg game is employed to model the strategic interactions.

Combined with the above references, it is easy to know that the game model is the most effective research tool for portraying the interaction relationship between the participants, but in the actual situation of the game model with multiple participants, it is often faced with the problems of insufficient information, hesitant decision-making behaviors of the parties, and insufficient trust of the participating parties towards each other. As a decentralized P2P network, blockchain can provide a safer and more efficient information transmission path for the parties involved in the game due to its decentralization, non-tampering, transparency, and smart contract features [18]. Leng J *et al.* [19] developed a difference-in-differences game model to analyze whether the application of clean energy and blockchain will have a positive effect on the ultimate benefits for decision makers. Ke Y *et al.* [20] proposed a novel Regional Electricity Trading Framework (RETF) based on consortium blockchain technology. The framework leverages the organizational structure of the consortium blockchain to enable secure and transparent transactions within the microgrid architecture, thereby increasing order turnover.

1.3. Main Contributions

Analyzing the research gaps in the aforementioned literature, this study designs a two-stage bi-level hybrid game model for VPP based on blockchain technology, considering the uncertainty of PV output. The hybrid game structure consists of cooperative–Stackelberg games. First, considering the impact of blockchain technology application on the revenue and electricity consumption utility of the three

parties—the MGO, the SESO, and the prosumer cluster—revenue models for all three are constructed. Subsequently, a DRO model based on the Wasserstein distance is developed and embedded into the revenue models of the MGO and the prosumers. Then, a bi-level hybrid game model for the VPP is established. The upper-level model is a distributed robust decision-making optimization model for the VPP and prosumers based on a Stackelberg game, while the lower-level model is a distributed robust operation optimization model for the VPP based on a cooperative game. As for the profit distribution within the VPP alliance, it is divided into two subproblems: the first is the problem of maximizing alliance profits, and the second is the problem of profit allocation, for which a symmetry-based Nash bargaining method is applied. Finally, numerical simulation experiments validate the effectiveness, scientific soundness, and rationality of the proposed method. Accordingly, the main contributions of this paper are summarized as follows:

1) The DRO model based on the Wasserstein metric effectively enhances the overall resilience of the system, *i.e.*, its risk resistance capability. By constructing an ambiguity set for uncertain variables, DRO optimizes the objective by considering the expected cost under the worst-case probability distribution within this set. Compared to traditional methods, it maintains strong performance even when data availability is limited.

2) The integration of blockchain technology enhances the revenue and electricity utility for all participants in electricity trading. Benefiting from the unique features of blockchain, namely smart contracts and distributed ledger technology, the electricity trading environment becomes more equitable and transparent. This reduces the decision-making costs for participants, thereby improving the overall operational efficiency of the system.

The remaining sections of the paper are organized as follows: In Section 2, the framework for hybrid gaming between the VPP and prosumers under blockchain technology was constructed and analyzed, along with an examination of the network architecture enabled by blockchain. Section 3 presents the distributed robust optimization model for the operational decision-making of the MGO and the operational model for the SESO, leading to the derivation of a distributed robust optimization model for VPP operational decisions. In Section 4, a distributed robust optimization model for prosumer operational decision-making is developed. Section 5 elaborates on the process for solving the hybrid game between the VPP and prosumers in a blockchain environment. Finally, Section 6 conducts numerical simulations using a practical case study and draws conclusive findings.

2. Hybrid Game Framework for Blockchain-Based VPP and Prosumer Alliance

This section will delineate the overall framework of the proposed study. Since all electricity-related transactions and scheduling operations are conducted on a blockchain trading platform, the blockchain-based network architecture of the system will also be elaborated following the introduction of the general framework.

2.1. System Framework

The system framework of the bi-level optimization model is shown in Figure 1.

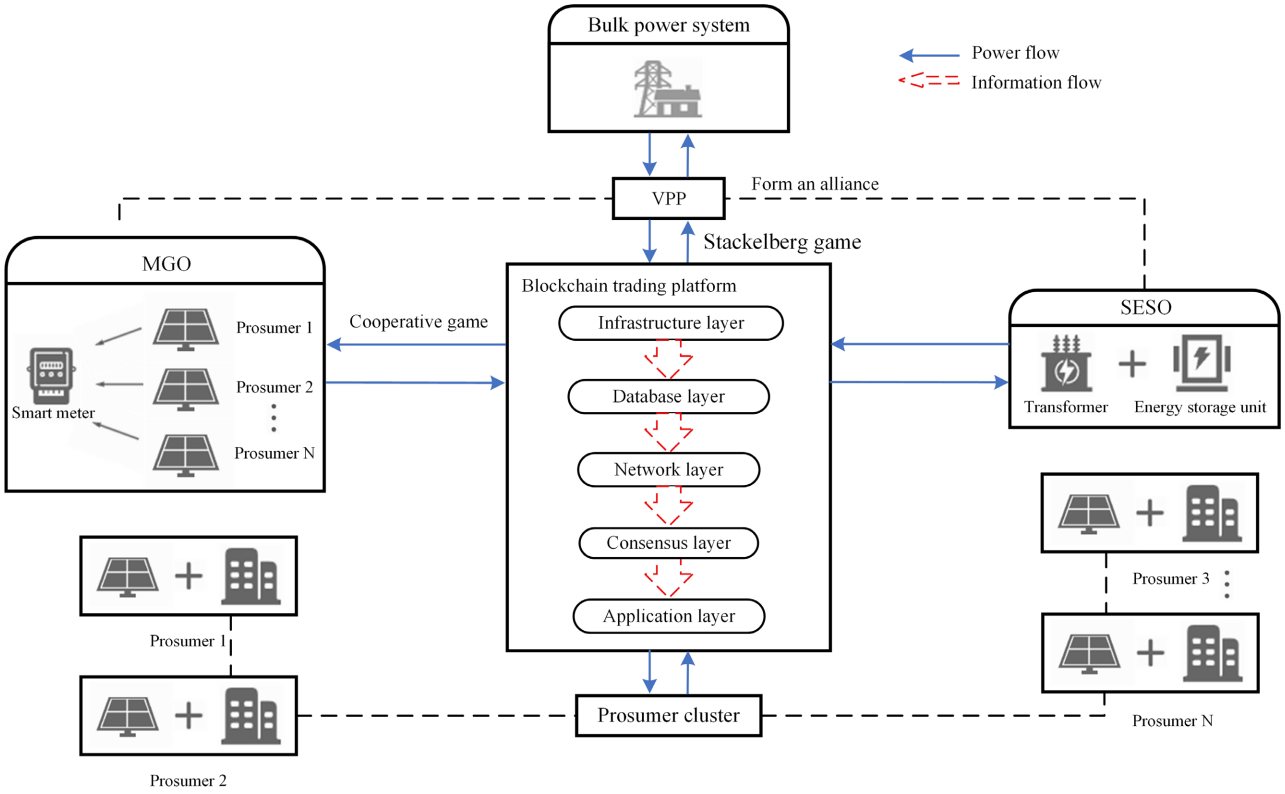

Figure 1. A system framework of virtual power plant based on blockchain technology counting and power trading.

As shown in Figure 1, the MGO monitors and manages the electricity production and consumption of the prosumer cluster through smart meters. To enhance the local consumption of PV power, increase system revenue, and balance internal electricity supply and demand, the MGO collaborates with the SESO to form a VPP alliance. This VPP alliance engages in electricity transactions with the lower-level prosumer alliance and the external bulk power system. When the electricity generated by prosumers is insufficient to meet their consumption demand during a specific period, the prosumers need to conduct electricity transactions with the VPP through the blockchain trading platform. To ensure that the prosumer alliance trades exclusively with the VPP, the internal purchase price must be lower than the price at which prosumers would directly purchase electricity from the bulk power system. Here, time-of-use (ToU) prices are used to describe the real-time market electricity prices, which are divided into peak, flat, and valley periods. Similarly, the internal selling price should be higher than the feed-in tariff for PV power. Within the VPP alliance, if the electricity generated by prosumers is less than the consumption during a certain period, the MGO needs to purchase electricity from the SESO; conversely, the MGO can also sell electricity to the SESO, resulting in interaction costs within the alliance.

2.2. Blockchain-Based System Network Architecture

The previous section described the operational mechanism of the model constructed in this study from a systemic perspective. This section will elucidate the role and advantages of the implemented blockchain trading platform. In traditional multi-participant hybrid game transaction models, it is challenging to ensure the security and fairness of information storage and interaction, the rationality of benefit distribution, and the efficiency of overall system management. Particularly in the electricity transaction model involving the VPP and the prosumer alliance established in this study, the MGO, SESO, and prosumers require a stable structured topology to operate more efficiently [21]. Blockchain technology, as a low-cost, high-efficiency, and highly reliable solution for information and data interaction, is highly compatible with the model developed in this study.

In the hybrid game model constructed in this paper, both the game equilibrium and the final operational mode of the system are achieved only after multiple decision-making iterations between the VPP and the prosumers. This process involves extensive distributed computations and requires such computations to be conducted under rules mutually agreed upon by all participating parties. Blockchain technology, through its distributed ledger operating under a consensus mechanism, leverages its immutability and security to efficiently store and process all electricity transaction data. Furthermore, it facilitates various transactions between the VPP and the prosumers via smart contracts, thereby optimizing system operation [22].

Based on the analysis of various game-theoretic models under blockchain technology in [18]-[22], it is evident that after participants in transactions or scheduling actively join the blockchain, their revenue or utility sees a certain degree of improvement compared to the pre-blockchain scenario. Combined with the earlier analysis, the application of blockchain technology in the model proposed in this study represents a proactive and justified endeavor. As illustrated in **Figure 2**, the VPP and the prosumer alliance, acting as physical layer in the blockchain, preprocess their fundamental data through basic equipment such as smart meters. This information is then transmitted to the infrastructure layer, data layer, network layer, consensus layer, and application layer of the blockchain's hierarchical architecture, ultimately forming the toolchain, transaction chain, and information chain within the blockchain trading platform. Among these, the toolchain ensures stable network conditions and efficient data transmission; the information chain records electricity-related data, resource allocation, and operational schedules of the VPP and individual prosumers; and the transaction chain provides computational support for formulating prices and contracts in the transaction market.

3. DRO Model for VPP Operation in Blockchain Environments

3.1. Constraints of the DRO Model

The Wasserstein distance is used to measure the distance between two probability

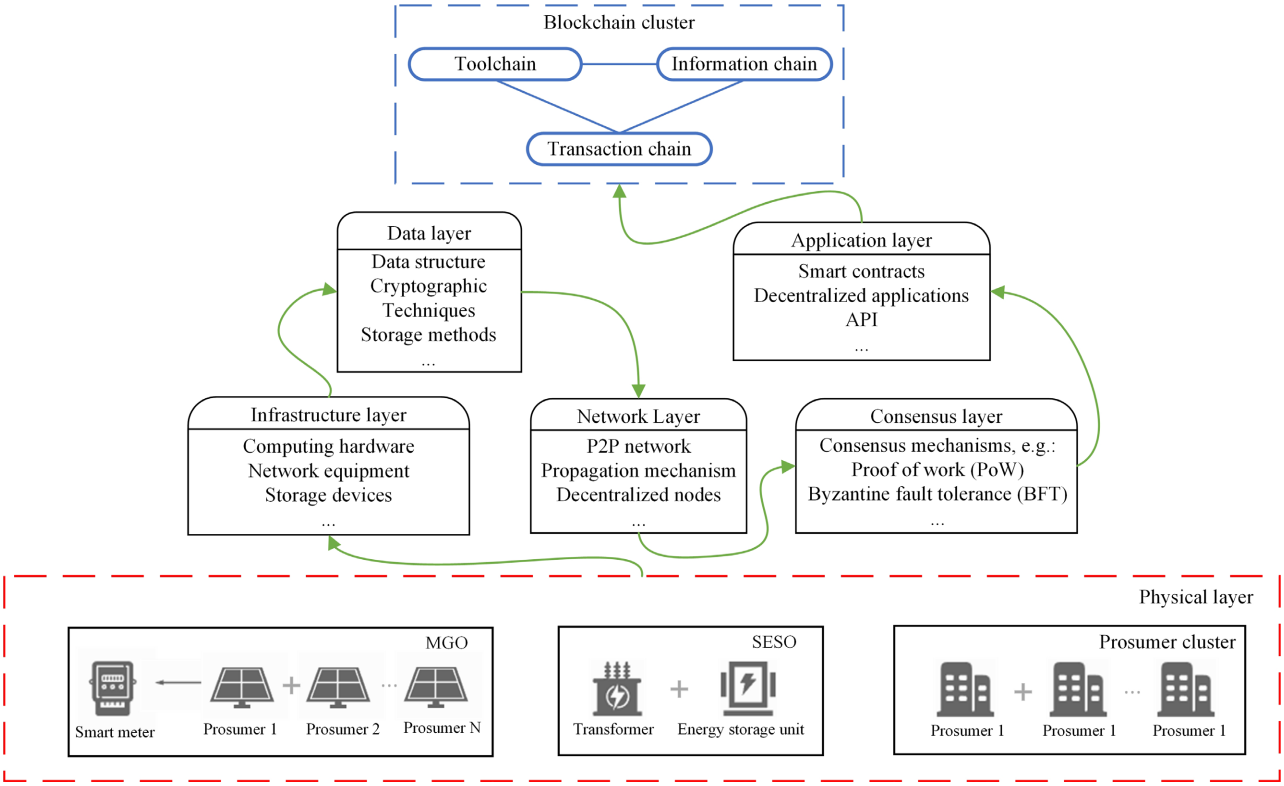

Figure 2. Blockchain-based system network architecture.

distributions. Compared to traditional distance/divergence measurement methods, the Wasserstein distance not only reflects differences in distribution shapes but also accounts for the geometric structure of the underlying space. Furthermore, it is better suited for handling scenarios with non-overlapping distributions or those requiring robust optimization, thereby endowing the DRO model with lower conservatism, *i.e.*, enhanced robustness.

First, the empirical distribution L_e is determined based on a sample set of $J=100$. The historical PV power output data is collected directly from the smart meters of the prosumers. Specifically, the data is sampled at a 1-hour resolution and aggregated across all prosumers for each time period. By using the aggregated total PV output rather than per-prosumer individual samples, the empirical distribution directly maps to the center of the Wasserstein ball, efficiently capturing the collective uncertainty of the prosumer cluster.

The set of total PV output values (the uncertain variable) for time period i is given by: $\left\{\sum_{n\in\chi_n} Q_{n,1}^{i,re}, \sum_{n\in\chi_n} Q_{n,2}^{i,re}, \sum_{n\in\chi_n} Q_{n,3}^{i,re}, \cdots, \sum_{n\in\chi_n} Q_{n,J}^{i,re}\right\}$. This empirical distribution serves as an estimate of the true distribution L. Then, due to the limited data volume of L_e, which makes it difficult to fully approximate L, a Wasserstein ball is constructed with L_e as the center and ε_{PV} as the radius. The true distribution L lies within this ball and satisfies: $\lim_{J\to\infty} L_e = L$. Finally, the Wasserstein distance is used to measure the distance between L_e and L, this measurement is employed to construct the ambiguity set.

The Wasserstein distance is defined as follows [23]:

$$d_W\left(L_e, L\right) = \inf_{P_{rf}} \int_{\Xi\times\Xi} \left\| \sum_{n\in\chi_n} Q_n^{i,ref} - \sum_{n\in\chi_n} Q_n^{i,re} \right\|_1 \Pi\left(\mathrm{d}\sum_{n\in\chi_n} Q_n^{i,ref}, \mathrm{d}\sum_{n\in\chi_n} Q_n^{i,re} \right) \quad (1)$$

where d_W represents the Wasserstein distance, L_e and L represent the reference distribution and the true distribution of the total PV output during time period i, respectively. P_{rf} denotes the probability that the joint sample distribution $\left(L_e, L\right)$ attains the samples $\left(\sum_{n\in\chi_n} Q_n^{i,ref}, \sum_{n\in\chi_n} Q_n^{i,re} \right)$. I represents the total number of time periods for electricity consumption, where $i \in \chi_i$, and $\chi_i = \{1,2,3,\cdots,I\}$. N is the total number of prosumers, where $n \in \chi_n$, and $\chi_n = \{1,2,3,\cdots,N\}$. Ξ denotes the support set range. Π is a joint distribution of $\sum_{n\in\chi_n} Q_n^{i,ref}$ and $\sum_{n\in\chi_n} Q_n^{i,re}$ with L_e and L, respectively. $\|\bullet\|_1$ denotes the L_1 norm, *i.e.*, the Manhattan distance.

Furthermore, the ambiguity set U_ε can be derived and is defined as follows:

$$U_\varepsilon = \left\{ P : d_W\left(L_e, L\right) \le \varepsilon_{PV} \right\} \quad (2)$$

where U_ε is precisely this Wasserstein ball with L_e as its center and ε_{PV} as its radius. P represents the probability distribution of all possible outcomes contained within a certain confidence level.

From **Equation (1)** and **Equation (2)**, we can derive the ambiguity set constraint concerning PV output uncertainty:

$$d_W\left(L_e, L\right) = \inf_{P_{rf}} \int_{\Xi\times\Xi} \left\| \sum_{n\in\chi_n} Q_n^{i,ref} - \sum_{n\in\chi_n} Q_n^{i,re} \right\|_1 \Pi\left(\mathrm{d}\sum_{n\in\chi_n} Q_n^{i,ref}, \mathrm{d}\sum_{n\in\chi_n} Q_n^{i,re} \right) \le \varepsilon_{PV} \quad (3)$$

$$P\left(dis_W\left(L_e, L\right) \le \varepsilon_{PV} \right) \ge \rho \quad (4)$$

where ρ represents a certain confidence level and ε_{PV} is the radius of the Wasserstein ball, which strictly controls the robustness of the DRO model based on the Wasserstein distance and satisfies $\lim_{J\to\infty} \varepsilon_{PV} = 0$.

Subsequently, based on [24], we can obtain an improved formula for calculating ε_{PV}:

$$\varepsilon_{PV} = K\sqrt{\frac{1}{J}}\Phi^{-1}\left(\rho\right) \quad (5)$$

where K is the adjustment factor. $\Phi^{-1}\left(\rho\right)$ is the ρ-th quantile of the standard normal distribution, compared to the traditional formula for calculating the Wasserstein ball radius, the above expression aligns more closely with the principles of the Central Limit Theorem and the Law of Large Numbers: 1) The distribution of the sample mean is asymptotically normal, 2) The estimation accuracy improves with the sample size.

The calculation formula for the adjustment factor K is:

$$K = \inf_{\sigma>0} 2\sqrt{\frac{1}{2\sigma}\left(1 + \ln\left(\frac{1}{J}\sum_{j=1}^{J} \mathrm{e}^{\sigma\left\| \sum_{n\in\chi_n} Q_{n,j}^{i,ref} - \widehat{\sum_{n\in\chi_n} Q_n^{i,re}} \right\|^2}\right)\right)} \quad (6)$$

where $\sigma > 0$ is the parameter to be optimized, $\sum_{n\in\chi_n} Q_{n,j}^{i,ref}$ is the j-th sample value in the empirical distribution L_e and $\widehat{\sum_{n\in\chi_n} Q_n^{i,re}}$ is the sample mean of the data.

A single Wasserstein radius ε_{PV} is applied across the entire scheduling horizon to maintain computational tractability and ensure a consistent risk-aversion level for the VPP operator. Regarding the dependence structure, the model assumes that the PV output uncertainty is temporally independent across the operational hours. However, spatial correlation among the prosumers is implicitly captured by constructing the ambiguity set based on the aggregated PV output and employing the L_1 norm in the Wasserstein metric definition.

3.2. A DRO Model for the MGO in Blockchain Environments

Acting as the regulator of the production and consumption activities of the prosumer alliance, the MGO collects data on the electricity consumption and generation of the prosumer alliance via the blockchain platform and conducts electricity transactions with both the prosumer alliance and the SESO. Let the electricity consumption of prosumer n in time period i be x_n^i, with $x_{n,\min}^i \le x_n^i \le x_{n,\max}^i$, where $x_{n,\min}^i$ and $x_{n,\max}^i$ are the minimum and maximum electricity consumption of prosumer n in period i, respectively. Let the electricity generation be Q_n^i with $Q_{n,\min}^i \le Q_n^i \le Q_{n,\max}^i$, where $Q_{n,\min}^i$ and $Q_{n,\max}^i$ are the minimum and maximum electricity generation of prosumer n in time period i, and $\sum_{n\in\chi_n} Q_n^i = \left\{ \sum_{n\in\chi_n} Q_{n,1}^{i,re}, \sum_{n\in\chi_n} Q_{n,2}^{i,re}, \sum_{n\in\chi_n} Q_{n,3}^{i,re}, \cdots, \sum_{n\in\chi_n} Q_{n,J}^{i,re} \right\} \in \Xi$. If $x_n^i > Q_n^i$, the prosumer purchases electricity from the MGO at the internal purchase price p_b^i. Conversely, if $x_n^i \le Q_n^i$, the prosumer sells electricity to the MGO at the internal selling price p_s^i. To ensure that prosumers are incentivized to trade exclusively with the MGO, the internal purchase and selling prices are set, respectively, lower than the ToU commercial electricity prices $p_{pk,bs}$, $p_{nr,bs}$, $p_{va,bs}$ for transactions with the main grid and higher than the PV feed-in tariff p_{ol}. Specifically, $p_{ol} \le p_s^i < p_b^i \le p_{pk,bs}$ during peak periods, $p_{ol} \le p_s^i < p_b^i \le p_{nr,bs}$ during flat periods, $p_{ol} \le p_s^i < p_b^i \le p_{va,bs}$ during valley periods. Consequently, the total electricity sold T_s^i and the total electricity purchased T_b^i in period i can be expressed as:

$$T_n^i = \begin{cases} \sum_{n\in\chi_s} \left(Q_n^i - x_n^i \right) \\ \sum_{n\in\chi_b} \left(x_n^i - Q_n^i \right) \end{cases} \tag{7}$$

where χ_s is the set of sellers among prosumers, $s \in \chi_s$, $\chi_s = \{1,2,3,\cdots,S\}$, χ_b is the set of buyers among prosumers, $b \in \chi_b$, $\chi_b = \{1,2,3,\cdots,B\}$, $\chi_s \subseteq \chi_n$, $\chi_b \subseteq \chi_n$, $\chi_s \cup \chi_b = \chi_n$ and $\chi_s \cap \chi_b = \varnothing$.

If $T_s^i > T_b^i$, the MGO needs to purchase electricity from the SESO to balance

internal supply and demand, if $T_s^i < T_b^i$, the MGO can sell excess electricity to the SESO. Both the MGO and SESO conduct electricity buying and selling through the interactive electricity price p_{co}^i. Operating to maximize its own profit, the MGO can derive its two-stage distributed robust optimization model based on Wasserstein as:

1) If $T_s^i > T_b^i$

$$\max_{p_{co}^i, p_n^i} \left\{ R_{MGO}^i = c_{co,s} + c_s + \inf_{P \in U_\varepsilon} \mathbb{E}_P \left[\mathbb{Q}\left(p_n^i, \sum_{n \in \chi_n} Q_n^i \right) \right] \right\} \tag{8}$$

2) If $T_s^i \le T_b^i$

$$\max_{p_{co}^i, p_n^i} \left\{ R_{MGO}^i = c_{co,b} + c_s + \inf_{P \in U_\varepsilon} \mathbb{E}_P \left[\mathbb{Q}\left(p_n^i, \sum_{n \in \chi_n} Q_n^i \right) \right] \right\} \tag{9}$$

where R_{MGO}^i represents the revenue of MGO in period i, $c_{co,s}$ and $c_{co,b}$ represent the cooperative game revenue between the MGO and SESO, *i.e.*, the interaction cost. c_s is the revenue from the MGO selling electricity to prosumers. $\mathbb{E}_P[\cdot]$ denotes the expected value operation on random variables, $\mathbb{Q}\left(p_n^i, \sum_{n \in \chi_n} Q_n^i \right)$ is the cost of real-time electricity purchasing due to the uncertainty of PV output. Its objective, within the ambiguity set U_ε based on the Wasserstein distance, is to minimize the expected revenue under the worst-case scenario distribution.

$c_{co,s}$ and $c_{co,b}$ are the interaction costs when the system is in a state of overall electricity selling and purchasing, respectively, and c_s is the MGO's revenue from electricity sales, specifically expressed as:

$$c_{co,s} = f(\theta) p_{co}^i P_{co,s}^i \tag{10}$$

$$c_{co,b} = -f^{-1}(\theta) p_{co}^i P_{co,b}^i \tag{11}$$

$$c_s = p_b^i \sum_{n \in \chi_b} x_n^i + p_s^i \sum_{n \in \chi_s} x_n^i \tag{12}$$

where p_{co}^i is the interactive electricity price between the MGO and SESO within the VPP alliance, $P_{co,s}^i$ and $P_{co,b}^i$ are the electricity quantity sold by the MGO to the SESO and the electricity quantity purchased by the MGO from the SESO, respectively, *i.e.*, the interactive electricity quantity between the two. $f(\theta)$ is the revenue loss function during electricity interaction before the application of blockchain technology. Based on the analysis in [18]-[22] and Section 2.2., due to the application of blockchain technology, its characteristics such as fairness and transparency of information can reduce most of the decision-making costs for transaction participants. Therefore, we can set the blockchain impact factor as:

$$f(\theta) = \frac{1}{e^{\theta(1-q)}} \tag{13}$$

where θ is the blockchain technology impact factor and $\theta \in [0,1]$, q is the on-chain rate, $q \in [0,1]$.

The blockchain impact factor $f(\theta)$ makes the benefits of blockchain opera-

tional by quantifying the reduction in specific frictional costs, such as information asymmetry and transaction verification overhead. The parameters can be calibrated using measurable transaction metrics: the on-chain rate q can be estimated by the historical ratio of transactions automatically settled via smart contracts to total transaction requests.

The real-time electricity purchase cost function is specifically expressed as:

$$\mathbb{Q}\left(p_n^i, \sum_{n\in\chi_n} Q_n^i\right) = -\left(p_b^i \sum_{n\in\chi_b} Q_n^i + p_s^i \sum_{n\in\chi_s} Q_n^i\right) \tag{14}$$

where $\sum_{n\in\chi_n} Q_n^i = \sum_{n\in\chi_s} Q_n^i + \sum_{n\in\chi_b} Q_n^i$.

Using strong duality theory and incorporating the dual form of the Wasserstein distance [25], the inner-layer mathematical expectation inf model can be further transformed into a maximization model:

$$\begin{aligned}&\inf_{P\in U_\varepsilon} E_P\left[\mathbb{Q}\left(p_n^i, \sum_{n\in\chi_n} Q_n^i\right)\right]\\ &= \max_{\lambda_1^i\geq 0}\left\{-\lambda_1^i\varepsilon_{PV} + \frac{1}{J}\sum_{j=1}^{J}\inf_{Q_n^i,\xi\in\Xi}\left(-\left(p_b^i \sum_{n\in\chi_b} Q_n^i + p_s^i \sum_{n\in\chi_s} Q_n^i\right) + \lambda_1^i\left\|\sum_{n\in\chi_n} Q_n^{i,re} - \sum_{n\in\chi_n} Q_{n,j}^{i,ref}\right\|\right)\right\}\end{aligned} \tag{15}$$

where λ_1^i is the Lagrange dual multiplier for the constraint that the electricity generation output in time period i is subject to ε_{PV}.

Finally, analyzing Equation (15), since the internal tariff satisfies the inequality $p_{ol} \le p_n^i \le p_{pk,bs}$, $p_s^i < p_b^i$, and $Q_n^i \ge 0$, therefore, the minimum value of the inner inf problem in Equation (15) can be expressed as:

$$\inf_{Q_n^i,\xi\in\Xi}\left(Q_n^i, p_n^i\right) = \begin{cases} -\left(p_b^i \sum_{n\in\chi_b} Q_{n,j}^{i,re} + p_s^i \sum_{n\in\chi_s} Q_{n,j}^{i,re}\right), & \lambda_1^i \ge p_b^i \\ -\infty, & \lambda_1^i < p_b^i \end{cases} \tag{16}$$

where $\sum_{n\in\chi_b} Q_{n,j}^{i,re}$ and $\sum_{n\in\chi_s} Q_{n,j}^{i,re}$ are the actual values of the j-th total PV output for the seller and buyer under the time period i.

Substituting Equation (16) back into Equation (15) gives:

$$\inf_{P\in U_\varepsilon} E_P\left[\mathbb{Q}\left(p_n^i, \sum_{n\in\chi_n} Q_n^i\right)\right] = \max_{\lambda_1^i\ge 0}\left\{-\lambda_1^i\varepsilon_{PV} + \frac{1}{J}\sum_{j=1}^{J} -\left(p_b^i \sum_{n\in\chi_b} Q_{n,j}^{i,re} + p_s^i \sum_{n\in\chi_s} Q_{n,j}^{i,re}\right)\right\} \tag{17}$$

To simplify the expression of the final DRO model of MGO, Equation (7) can be first transformed into:

$$\overline{T}_n^{i,re} = \begin{cases} \frac{1}{J}\sum_{j=1}^{J}\sum_{n\in\chi_s}\left(Q_{n,j}^{i,re} - x_n^i\right) \\ \frac{1}{J}\sum_{j=1}^{J}\sum_{n\in\chi_b}\left(x_n^i - Q_{n,j}^{i,re}\right) \end{cases} \tag{18}$$

Finally, by bringing Equation (18) back to the original Equations (8) and (9), we can obtain the final MGO DRO model as:

$$\max_{p_n^i,\lambda_1^i,p_{co}^i}\left\{R_{MGO}^i\left(\lambda_1^i,p_n^i,p_{co}^i\right)=\begin{cases}\overline{T}_b^{i,re}p_b^i-\overline{T}_s^{i,re}p_s^i+f\left(\theta\right)p_{co}^i\left(\overline{T}_s^{i,re}-\overline{T}_b^{i,re}\right)-\lambda_1^i\varepsilon_{PV}, & \overline{T}_s^{i,re}>\overline{T}_b^{i,re},\lambda_1^i\geq p_b^i\\ \overline{T}_b^{i,re}p_b^i-\overline{T}_s^{i,re}p_s^i+f^{-1}\left(\theta\right)p_{co}^i\left(\overline{T}_s^{i,re}-\overline{T}_b^{i,re}\right)-\lambda_1^i\varepsilon_{PV}, & \overline{T}_s^{i,re}\leq\overline{T}_b^{i,re},\lambda_1^i\geq p_b^i\end{cases}\right\} \quad (19)$$

3.3. Revenue Optimization Model for SESO under Blockchain Technology

Before joining the VPP alliance, the SESO bought electricity at the off-peak real-time market price p_{val} and sold it at the peak real-time market price p_{peek} to profit from the price difference. However, the peak and off-peak prices in the real-time market are highly volatile and unstable. After forming a VPP alliance with the MGO, transactions with downstream prosumers become more stable and controllable. Additionally, we assume that the energy storage capacity of the SESO far exceeds the electricity demand of the prosumer group. And, the charging and discharging power P_{ch}^i and P_{dis}^i represent exclusively the electricity exchanged between the MGO and the SESO. Moreover, during electricity interaction with the MGO, the SESO has already stored a substantial amount of electricity. The operational revenue model of the SESO is as follows:

$$\begin{aligned}R_{SESO}^i=&\left(f\left(\theta\right)p_{co}^i-p_{val}/\eta_{dis}\eta_{ch}\right)P_{dis}^i+\left(p_{peek}\eta_{dis}\eta_{ch}-f^{-1}\left(\theta\right)p_{co}^i\right)P_{ch}^i\\&-\left(P_{dis}^i+P_{ch}^i\right)\eta_{om}\end{aligned} \quad (20)$$

$$\text{s.t.}\begin{cases}S_{\min}\leq S^i\leq S_{\max}\\ E_{\min}\leq E^i\leq E_{\max}\\ 0\leq P_{ch}^i\leq uP_{ch,\max}^i\\ 0\leq P_{dis}^i\leq\left(1-u\right)P_{dis,\max}^i\\ S^i=\left(E_{\max}S^{i-1}+\eta_{ch}P_{ch}^i-P_{dis}^i/\eta_{dis}\right)/E_{\max}\end{cases} \quad (21)$$

where R_{SESO}^i represents the revenue of SESO in period i, P_{dis}^i and P_{ch}^i represent the discharge and charge power of the energy storage system in time period i, respectively, $P_{ch,\max}^i$ and $P_{dis,\max}^i$ denotes the maximum charge and discharge power of the energy storage system in time period i, η_{om} is the operation and maintenance coefficient for the SESO's charging and discharging, where $\eta_{om}\in\left[0,1\right]$. S^i represents the state of charge (SOC) of the energy storage system in time period i, while $S_{\min}$ and $S_{\max}$ are the lower and upper limits of the SOC. E^i denotes the energy state of the energy storage system in time period i, with $E_{\min}$ and $E_{\max}$ being the lower and upper limits of the energy state. u is a Boolean variable introduced to prevent the energy storage system from simultaneously charging and discharging in any given time period. η_{ch} and η_{dis} represent the charging and discharging efficiencies of the energy storage system, where $\eta_{ch}\in\left[0,1\right]$ and $\eta_{dis}\in\left[0,1\right]$.

3.4. DRO Model for VPP Operation

After the MGO and SESO form an alliance, the VPP operates to maximize the alliance's revenue *i.e.*,

$$\max_{p_n^i,\lambda_1^i,p_{co}^i}\left\{R_{VPP}^i\left(\lambda_1^i,p_n^i\right)=R_{MGO}^i\left(\lambda_1^i,p_n^i,p_{co}^i\right)+R_{SESO}^i\left(p_{co}^i\right)\right\} \tag{22}$$

where R_{VPP}^i represents the revenue of VPP in period i, the electricity exchange costs between the two parties offset each other, and the internal electricity supply meets the balance: $\overline{T}_b^{i,re}+P_{dis}^i+P_{co,s}^i=\overline{T}_s^{i,re}+P_{ch}^i+P_{co,b}^i$. By integrating Equations (19)-(22), we can derive the DRO model for the VPP as follows:

1) $\overline{T}_s^{i,re}>\overline{T}_b^{i,re}$:

$$\max_{p_n^i,\lambda_1^i}\left\{R_{VPP}^i\left(\lambda_1^i,p_n^i\right)=\overline{T}_b^{i,re}p_b^i-\overline{T}_s^{i,re}p_s^i+p_{peek}\eta_{dis}\eta_{ch}P_{ch}^i-P_{ch}^i\eta_{om}-\lambda_1^i\varepsilon_{PV}\right\} \tag{23}$$

$$\text{s.t.}\begin{cases}\overline{T}_s^{i,re}>\overline{T}_b^{i,re}\\ \lambda_1^i\geq p_b^i\\ p_{ol}\leq p_s^i<p_b^i\leq p_{pk,bs}\\ x_{n,\min}^i\leq x_n^i\leq x_{n,\max}^i\\ S_{\min}\leq S^i\leq S_{\max}\\ E_{\min}\leq E^i\leq E_{\max}\\ 0\leq P_{ch}^i\leq P_{ch,\max}^i\\ S^i=\left(E_{\max}S^{i-1}+\eta_{ch}P_{ch}^i-P_{dis}^i/\eta_{dis}\right)/E_{\max}\end{cases} \tag{24}$$

2) $\overline{T}_s^{i,re}\leq\overline{T}_b^{i,re}$:

$$\max_{p_n^i,\lambda_1^i}\left\{R_{VPP}^i\left(\lambda_1^i,p_n^i\right)=\overline{T}_b^{i,re}p_b^i-\overline{T}_s^{i,re}p_s^i-p_{val}/\eta_{dis}\eta_{ch}P_{dis}^i-P_{dis}^i\eta_{om}-\lambda_1^i\varepsilon_{PV}\right\} \tag{25}$$

$$\text{s.t.}\begin{cases}\overline{T}_s^{i,re}\leq\overline{T}_b^{i,re}\\ \lambda_1^i\geq p_b^i\\ p_{ol}\leq p_s^i<p_b^i\leq p_{pk,bs}\\ x_{n,\min}^i\leq x_n^i\leq x_{n,\max}^i\\ S_{\min}\leq S^i\leq S_{\max}\\ E_{\min}\leq E^i\leq E_{\max}\\ 0\leq P_{dis}^i\leq P_{dis,\max}^i\\ S^i=\left(E_{\max}S^{i-1}+\eta_{ch}P_{ch}^i-P_{dis}^i/\eta_{dis}\right)/E_{\max}\end{cases} \tag{26}$$

4. DRO Model for Prosumer Operation under Blockchain Technology

Prosumers as the lower-level followers in the Stackelberg game, engage in a game with the upper-level VPP alliance to maximize their own electricity consumption utility. The goal is to determine the optimal electricity consumption that maximizes their utility under the optimized pricing strategy set by the VPP alliance. Based on [26]-[29] regarding electricity consumption utility on the demand side, most existing research uses quadratic functions or natural logarithmic functions $\alpha\ln(1+x)$ to model demand-side electricity utility. This study, drawing on extensive literature and experimental analysis, adopts the inverse hyperbolic sine

function $\alpha\text{arsinh}(x)$ to model prosumer electricity utility. Compared to $\alpha\ln(1+x)$, the core advantages of $\alpha\text{arsinh}(x)$: 1) When users face situations where the cost of electricity consumption exceeds the utility, $\alpha\text{arsinh}(x)$ allows zero consumption to be an optimal solution of the model, which aligns better with real-world scenarios; 2) The second derivative of $\alpha\text{arsinh}(x)$ smoothly transitions to zero at the origin, which enhances the numerical stability and convergence speed of the algorithm. Based on this, and considering Equations (3) and (4) along with the analysis of the MGO's distributed robust optimization model in Section 3.2., the detailed construction of the prosumer's distributed robust model for electricity utility will not be elaborated further.

In the generic utility formulation $\alpha\text{arsinh}(x)$, the parameter α represents the general marginal utility coefficient, which dictates a prosumer's sensitivity to electricity consumption increments. In our proposed DRO model for a prosumer electricity utility, this parameter is specifically denoted as $k_{n,blo}^{i}$ to capture the time-varying, prosumer-specific preference under blockchain technology. These utility parameters are calibrated based on historical consumption elasticity, ensuring that the modeled utility curve reflects realistic comfort constraints—namely, that the marginal benefit of electricity consumption gradually diminishes as a prosumer's basic comfort needs are satisfied.

The distributed robust optimization model for prosumer electricity utility under blockchain technology is as follows:

$$\max_{\lambda_2^i,\lambda_3^i,x_n^i}\left\{\sum_{n\in\chi_n}U_n^i\left(\lambda_2^i,\lambda_3^i,x_n^i\right)=\begin{cases}\sum\limits_{n\in\chi_b}\left(k_{n,blo}^{i}\text{arsinh}\left(x_n^i\right)-p_b^i\left(x_n^i-\dfrac{1}{J}\sum\limits_{j=1}^{J}Q_{n,j}^{i,re}\right)-\lambda_2^i\varepsilon_{PV}\right), & n\in\chi_b,\lambda_2^i\geq p_b^i\\ \sum\limits_{n\in\chi_s}\left(k_{n,blo}^{i}\text{arsinh}\left(x_n^i\right)-p_s^i\left(x_n^i-\dfrac{1}{J}\sum\limits_{j=1}^{J}Q_{n,j}^{i,re}\right)-\lambda_3^i\varepsilon_{PV}\right), & n\in\chi_s,\lambda_3^i\geq p_s^i\end{cases}\right\} \tag{27}$$

where U_n^i represents the utility of prosumers in time period i, λ_2^i and λ_3^i are the Lagrange dual multipliers for the electricity generation constraints of prosumers (buyers and sellers, respectively) under the ε_{PV} constraint during time period i, $\frac{1}{J}\sum_{n\in\chi_s}\sum_{j=1}^{J}Q_{n,j}^{i,re}+\frac{1}{J}\sum_{n\in\chi_b}\sum_{j=1}^{J}Q_{n,j}^{i,re}=\frac{1}{J}\sum_{n\in\chi_n}\sum_{j=1}^{J}Q_{n,j}^{i,re}$ and $k_{n,blo}^{i}$ represents the electricity preference coefficients of prosumers under blockchain technology in time period i, according to [19], the coefficient can be set as follows:

$$k_{n,blo}^{i}=\begin{cases}\dfrac{k_{n,0}^{i}}{e^{Aq}}, & n\in\chi_s\\ e^{Aq}k_{n,0}^{i}, & n\in\chi_b\end{cases} \tag{28}$$

where $k_{n,0}^{i}$ represents the initial electricity consumption preference of the prosumer n in time period i without considering blockchain; A is the impact factor of blockchain on the prosumer's electricity consumption preference and $A\in[0,1]$.

Similarly, the impact factor A can be calibrated based on the empirically observed increase in prosumer trading preferences following the reduction in settle-

ment risks provided by the distributed ledger.

5. Solution for Hybrid Game Model

The model constructed in this study consists of an upper-level VPP DRO operation model and a lower-level prosumer alliance DRO model, forming a cooperative-Stackelberg-cooperative hybrid game model. The model involves multiple layers of internal and external nesting with numerous parameters to be optimized, making direct solution complex and challenging to directly identify the final optimal solution that fits all optimization models. Therefore, this paper adopts the ADMM algorithm [30]. First, the upper-level VPP DRO operation model is decomposed into two subproblems: (Q1) VPP alliance revenue maximization problem, and (Q2) VPP alliance revenue distribution problem based on symmetric Nash bargaining. Q1 engages in a Stackelberg game with the lower-level prosumer alliance, while Q2 simultaneously conducts internal cooperative bargaining with the lower-level prosumer alliance.

5.1. Solution for Stackelberg Game Model

The Stackelberg game, as an efficient method for resolving transaction and scheduling issues between two entities, serves as an ideal tool for achieving balanced coexistence between the VPP alliance and the prosumer alliance in this study. The Stackelberg game consists of three elements: game participants, game objectives, and game strategies. In this paper, these three elements can be specifically defined as:

1) Game participants: The upper-level VPP alliance and the lower-level prosumer alliance;

2) Game objectives: Both parties engage in the game with the goal of optimizing their respective DRO models. The upper-level VPP alliance aims for $\max_{p_n^i,\lambda_1^i} R_{VPP}^i\left(\lambda_1^i, p_n^i\right)$; the lower-level prosumer alliance seeks $\max_{\lambda_2^i,\lambda_3^i,x_n^i} \sum_{n\in\chi_n} U_n^i\left(\lambda_2^i,\lambda_3^i,x_n^i\right)$.

3) Game Strategies: The upper-level VPP alliance uses the formulation of internal electricity purchase/selling prices and Lagrange dual multipliers as its strategy set: $s_{VPP}=\left\{p_b^i,p_s^i,\lambda_1^i \middle| p_b^i,p_s^i\in\mu,\lambda_1^i\geq p_b^i\right\}$; The lower-level prosumer alliance uses its electricity consumption and Lagrange dual multipliers as its strategy set: $s_{pro}=\left\{x_n^i,\lambda_2^i,\lambda_3^i \middle| x_n^i\in\chi_{pro},\lambda_2^i\geq p_b^i,\lambda_3^i\geq p_s^i\right\}$, where, χ_{pro} is the set of all possible electricity consumption scenarios for prosumers.

This Stackelberg game model is guaranteed to have an equilibrium solution. For the proof of solution existence, please refer to Appendix A. This study employs the backward induction method to solve the aforementioned model. The final game equilibrium solution must satisfy the following conditions:

$$R_{VPP}^i\left(p_b^{i*},p_s^{i*},\lambda_1^{i*}\right)\geq R_{VPP}^i\left(p_b^i,p_s^i,\lambda_1^i\right)\quad \forall p_n^i\in\mu\setminus\left\{p_b^{i*},p_s^{i*}\right\},\forall\lambda_1^i\geq p_b^i\in\mu\setminus\left\{p_b^{i*}\right\} \tag{29}$$

$$U_n^i\left(x_n^{i*},\lambda_2^{i*},\lambda_3^{i*}\right)\geq U_n^i\left(x_n^i,\lambda_2^i,\lambda_3^i\right)\quad \forall x_n^i\in\chi_{pro}\setminus\left\{x_n^{i*}\right\},\forall\lambda_2^i\geq p_b^i\in\mu\setminus\left\{p_b^{i*}\right\},\forall\lambda_3^i\geq p_s^i\in\mu\setminus\left\{p_s^{i*}\right\} \tag{30}$$

where μ represents the distribution of internal electricity prices.

5.2. Solution Method for Cooperative Game Model

VPP Alliance Cooperative Game Model Solution

A necessary condition for parties engaged in a game to form a coalition is that the benefits achieved through cooperation must exceed the sum of their individual benefits obtained independently. This principle is known as superadditivity, in this study, this property should be manifested as follows, which detailed proof is provided in Appendix B.

$$R_{VPP}^{i}\left(\lambda_1^i, p_n^i\right) \geq R_{SESO,0}^{i} + R_{MGO,0}^{i} \tag{31}$$

Nash bargaining, as a pivotal concept in game theory, is frequently employed to address the equitable distribution of cooperation benefits among multiple participants in cooperative games. This study adopts a cooperative game model based on symmetric Nash bargaining theory to allocate the cooperative surplus within the upper-level VPP alliance. The specific model is as follows [31]:

$$\begin{cases} \max\limits_{p_{co}^i} \left(R_{SESO}^{i} - R_{SESO,0}^{i}\right)\left(R_{MGO}^{i} - R_{MGO,0}^{i}\right) \\ \text{s.t.} \quad R_{SESO}^{i} \geq R_{SESO,0}^{i}, R_{MGO}^{i} \geq R_{MGO,0}^{i} \end{cases} \tag{32}$$

where $R_{SESO,0}^{i}$ and $R_{MGO,0}^{i}$ represent the revenues of the two parties in time period i when they do not form an alliance.

To facilitate the solution of the model and based on the above analysis, this model is divided into two subproblems, Q1 and Q2, for solving. The specific forms are as follows:

Q1) VPP alliance revenue maximization problem

$$\begin{cases} \max\limits_{p_n^i, \lambda_1^i} R_{VPP}^{i}\left(\lambda_1^i, p_n^i\right) \\ \text{s.t.} \quad \text{Eqs. (24), (26)} \end{cases} \tag{33}$$

Q2) VPP alliance cooperative surplus distribution problem

1) $\overline{T}_s^{i,re} > \overline{T}_b^{i,re}$

$$\begin{cases} \max\limits_{p_{co}^i} \ln\left(\left(\eta_{dis}\eta_{ch}p_{peek} - f^{-1}(\theta)p_{co}^i\right)P_{ch}^{i*} - P_{ch}^{i*}\eta_{om} - R_{SESO,0}^{i}\right) \\ \quad + \ln\left(\left(\overline{T}_b^{i,re}p_b^{i*} - \overline{T}_s^{i,re}p_s^{i*} + f(\theta)p_{co}^i\left(\overline{T}_s^{i,re} - \overline{T}_b^{i,re}\right) - \lambda_1^{i*}\varepsilon_{PV}\right) - R_{MGO,0}^{i}\right) \\ \text{s.t.} \quad \left(\eta_{dis}\eta_{ch}p_{peek} - f^{-1}(\theta)p_{co}^i\right)P_{ch}^{i*} - P_{ch}^{i*}\eta_{om} \geq R_{SESO,0}^{i} \\ \qquad \overline{T}_b^{i,re}p_b^{i*} - \overline{T}_s^{i,re}p_s^{i*} + f(\theta)p_{co}^i\left(\overline{T}_s^{i,re} - \overline{T}_b^{i,re}\right) - \lambda_1^{i*}\varepsilon_{PV} \geq R_{MGO,0}^{i} \end{cases} \tag{34}$$

2) $\overline{T}_s^{i,re} \leq \overline{T}_b^{i,re}$

$$\begin{cases} \max\limits_{p_{co}^i} \ln\left(\left(f(\theta)p_{co}^i - p_{val}/\eta_{dis}\eta_{ch}\right)P_{dis}^{i*} - P_{dis}^{i*}\eta_{om} - R_{SESO,0}^{i}\right) \\ \quad + \ln\left(\left(\overline{T}_b^{i,re}p_b^{i*} - \overline{T}_s^{i,re}p_s^{i*} + f^{-1}(\theta)p_{co}^i\left(\overline{T}_s^{i,re} - \overline{T}_b^{i,re}\right) - \lambda_1^{i*}\varepsilon_{PV}\right) - R_{MGO,0}^{i}\right) \\ \text{s.t.} \quad \left(f(\theta)p_{co}^i - p_{val}/\eta_{dis}\eta_{ch}\right)P_{dis}^{i*} - P_{dis}^{i*}\eta_{om} \geq R_{SESO,0}^{i} \\ \qquad \overline{T}_b^{i,re}p_b^{i*} - \overline{T}_s^{i,re}p_s^{i*} + f^{-1}(\theta)p_{co}^i\left(\overline{T}_s^{i,re} - \overline{T}_b^{i,re}\right) - \lambda_1^{i*}\varepsilon_{PV} \geq R_{MGO,0}^{i} \end{cases} \tag{35}$$

where the values marked with "$*$" are the optimal values obtained after the Stackel-

berg game between Equations (22) and (27).

5.3. Algorithm Design

Figure 3 illustrates the solution process of the two-stage bi-level ADMM model, with the specific steps as follows:

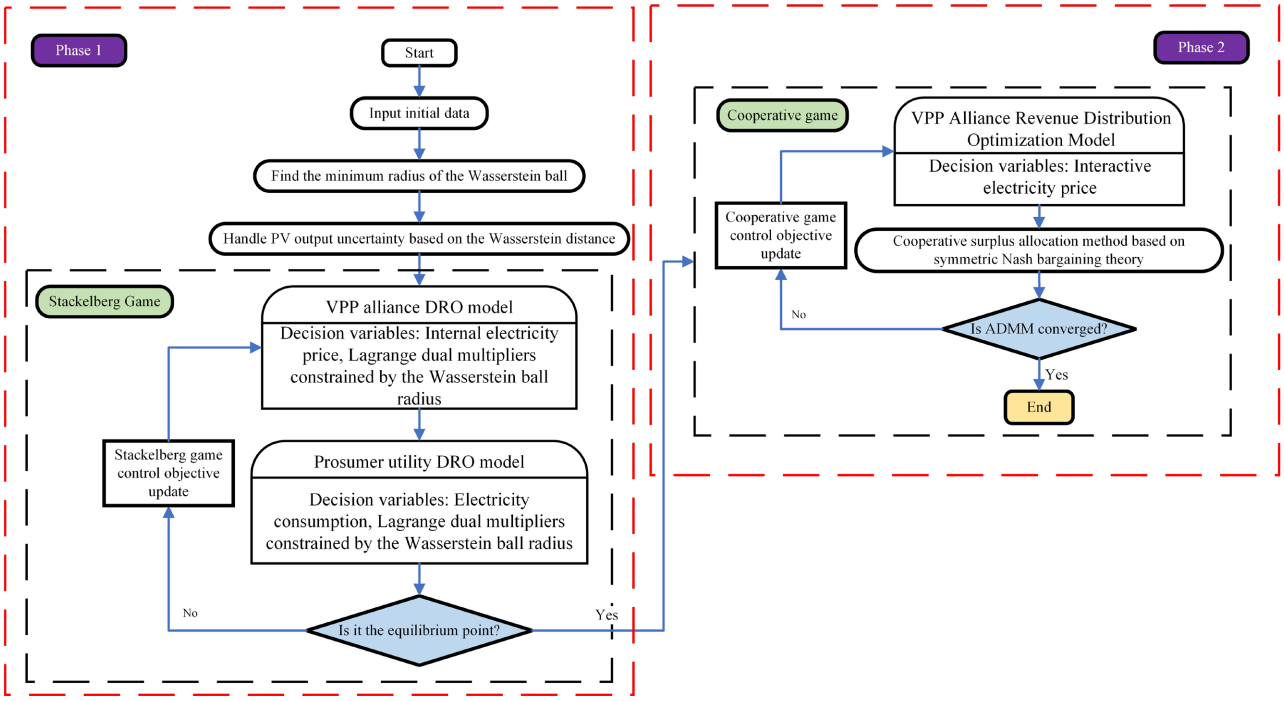

Figure 3. Two-stage two-layer virtual power plant optimization operation model solution process.

1) Input initial data, such as prosumers' initial electricity consumption, initial generation output, the empirical distribution derived from PV reference output values, real-time market ToU electricity prices, and other initial parameters.

2) Determine the minimum radius of the Wasserstein ball based on the empirical distribution and use it to handle PV uncertainty.

3) Substitute the initial values into Equations (23) and (27), and conduct a Stackelberg game between Equation (23) (representing the VPP alliance's robust optimization model) and Equation (27) (representing the prosumers' robust optimization model). Iterate repeatedly until the game equilibrium point is found.

4) Substitute the optimal decision variables obtained from the Stackelberg game into Equations (34) and (35). Use the symmetry-based Nash bargaining method to allocate the cooperative surplus between the MGO and SESO in the VPP alliance. Iterate repeatedly until the optimal interactive electricity price and the optimal allocation scheme are determined.

5) The ADMM-based iterative process terminates when the monitored residuals fall below the predefined convergence tolerances, or when the maximum iteration limit $k_{\max}$ is reached. Specifically, the algorithm monitors two quantitative indicators at each iteration k: the primal residual r^k, which reflects the mis-

match in the expected energy transaction quantities between the VPP and the prosumers, and the dual residual s^k, which measures the step-to-step variation in the consensus pricing variables. The iterations stop and the equilibrium is guaranteed when both $\left\|r^k\right\|_2 \le \varepsilon^{pri}$ and $\left\|s^k\right\|_2 \le \varepsilon^{dual}$ are satisfied.

6. Numerical Simulation

The numerical simulation of the model constructed in this study was conducted on Matlab R2018a, using actual data from multiple commercial buildings in a certain region of China as a case study. The number of prosumers was set to 8, with 1 MGO and 1 SESO. Considering the effective time period of PV output, the daily hours from 7:00 to 19:00 were selected for the study. The value of parameters are shown in Table 1. The initial electricity consumption and generation output of prosumers on a typical day are shown in Figure 4 and Figure 5, respectively.

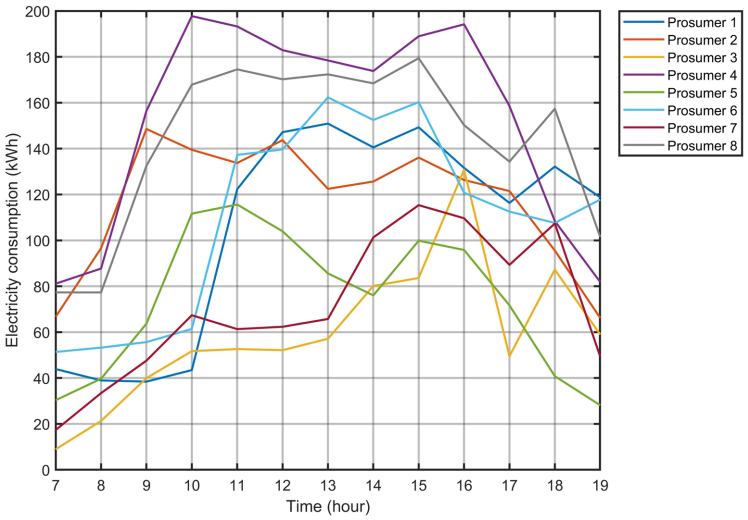

Figure 4. Initial electricity consumption by prosumers.

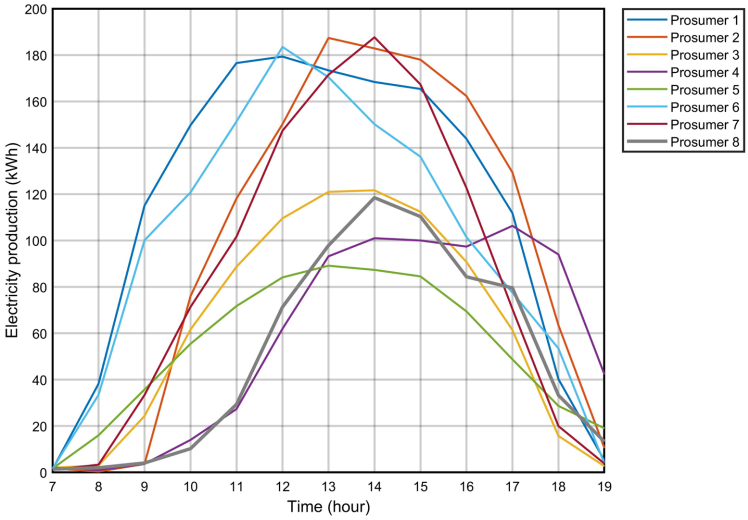

Figure 5. Initial electricity production by prosumers.

Table 1. The value of other parameters.

Parameter	Value
ρ	0.9
J	100
N	8
θ	0.1
A	0.1
η_{om}	0.1
η_{ch}	0.98
η_{dis}	0.98
$p_{bs,pk}$	1.2/CNY/kWh
$p_{bs,nor}$	0.8/CNY/kWh
p_{peek}	0.8/CNY/kWh
p_{val}	0.3/CNY/kWh
p_{ol}	0.3/CNY/kWh
σ_{car}	0.879
$k_{\max}$	300
ε^{pri}	10^{-3}
ε^{dual}	10^{-3}

Based on the temporal variations of prosumers' electricity consumption and generation shown in Figure 4 and Figure 5, this study defines the off-peak electricity consumption periods as 7:00-9:00 and 17:00-19:00, and the peak electricity consumption period as 10:00-16:00.

6.1. Analysis of System Optimization Decision Schemes

To verify the positive impact of the model constructed in this paper on system operation, the following four schemes are established for comparative analysis. Among them, "①", "②", "③", and "④" respectively represent: ① whether the MGO and SESO engage in a cooperative game based on symmetric Nash bargaining; ② whether to join the blockchain trading platform; ③ whether to consider the uncertainty of PV output; ④ whether the VPP alliance/MGO conducts a Stackelberg game with the prosumers. The details are shown in Table 2.

Table 2. Schemes settings.

Scheme	①	②	③	④
1	✓	✓	✓	✓

Continued

2	✓	×	✓	✓
3	✓	✓	×	✓
4	×	✓	✓	×
5	×	✓	✓	✓

It should be noted that when the MGO and SESO choose not to engage in a cooperative game, the revenue of the SESO comes from arbitrage in the real-time electricity market, and the electricity quantity traded with the main grid is the same as that traded between the MGO and the prosumers.

Through numerical experiments, we can obtain data such as the revenues of the MGO and SESO and the system carbon emissions under different schemes. We assume that during any time period when the total electricity consumption of prosumers exceeds their total generation, requiring the MGO to purchase electricity from the SESO to balance internal supply and demand, the electricity stored by the SESO is partially procured from the main grid and partially purchased from the MGO. The portion procured from the main grid originates exclusively from thermal power generation. For Schemes 1 - 3, carbon emissions are characterized using Equation (36), while for Schemes 4 and 5, Equation (37) is employed. The details are shown in Table 3.

Table 3. VPP alliance benefits and prosumers' electricity utility.

Scheme	MGO revenue/CNY	SESO revenue/CNY	Local PV consumption rate	Prosumer electricity utility/CNY	Carbon emissions/Ton
1	1500.881	1937.293	100%	46858.331	2483.127
2	985.169	1291.138	100%	43144.273	2391.995
3	1699.277	2031.646	100%	47469.146	2313.601
4	1001.386	1750.74	50.3%	45961.562	3124.631
5	1293.729	1750.74	56.7%	46076.327	2858.299

$$O_{car}^{i} = \sigma_{car} \max\left\{ \max\left(\sum_{n\in\chi_n} \left(x_n^i - \frac{1}{J}\sum_{j=1}^{J} Q_{n,j}^{i,re} \right), 0 \right) - \max\left(\eta_{dis}\eta_{ch} \sum_{t=1}^{i-1} \sum_{n\in\chi_n} \left(\frac{1}{J}\sum_{j=1}^{J} Q_{n,j}^{i-1,re} - x_n^{i-1} \right), 0 \right), 0 \right\} \tag{36}$$

$$O_{car}^{i} = \sigma_{car} \max\left(\sum_{n\in\chi_n} \left(x_n^i - \frac{1}{J}\sum_{j=1}^{J} Q_{n,j}^{i,re} \right), 0 \right) \tag{37}$$

where O_{car}^{i} represents the carbon emissions of the system during time period i, σ_{car} is the carbon emission factor for thermal power generation.

As shown in Table 3, the operational status of the system under various decision schemes composed of different possibilities can be observed in detail. Scheme 1, which incorporates cooperative game + blockchain technology + uncertainty management + Stackelberg game, represents the most technologically comprehensive operational model. Scheme 2 lacks the application of blockchain technology and is used to evaluate the marginal contribution of blockchain. Scheme 3 reflects the upper limit of system performance under the most idealized conditions, demonstrating the cost of risk management. Scheme 4 lacks a cooperative mechanism and also does not consider the Stackelberg game mechanism between the VPP alliance and the prosumers, primarily reflecting the impact of the hybrid game mechanism on the system. Scheme 5 does not consider the cooperative mechanism, with the main purpose of evaluating the marginal contribution of the cooperative mechanism.

By comparing Schemes 1, 4, and 5, it can be observed that under the hybrid game mechanism, the revenues of the MGO and SESO in the VPP alliance increased by 499.495 CNY and 186.553 CNY, respectively. Additionally, the local PV consumption rate reached 100% in Scheme 1, while the electricity utility of prosumers improved by 896.769 CNY and 1982.004 CNY compared to Schemes 4 and 5. This demonstrates that the hybrid game mechanism effectively enhances alliance revenues, prosumers' electricity utility, and promotes system operational efficiency and environmental benefits.

A comparison between Schemes 1 and 2 reveals that, under the consideration of blockchain technology, the revenues and electricity utility of the MGO, SESO, and prosumers increased by over 40%. This is attributed to the unique features of blockchain technology, such as distributed ledgers and smart contracts, which ensure transaction transparency and fairness, significantly reduce the costs of electricity interactions, and improve the efficiency of electricity trading and scheduling.

Comparing Schemes 1 and 3, after accounting for the uncertainty of PV output, the revenues and utility of decision-makers and prosumers decreased. This is because decision-makers, considering the uncertainty of risks, implemented risk management to enhance system resilience. Although this reduced revenues, it strengthened their risk resistance, mitigated potential future economic losses, and further improved the stability of system operation.

Comparing Schemes 1, 3, and 5, in Scheme 5, where no cooperative alliance was considered, the MGO still engaged in a Stackelberg game with prosumers to determine internal electricity prices. However, the MGO's revenue was significantly lower than the results achieved in Schemes 1 and 3, which considered cooperative gaming. This confirms that cooperative gaming is key to maximizing benefits and achieving efficient allocation.

Based on the carbon emissions data in Table 3, the five schemes perform as follows, Scheme 4 has the highest carbon emissions (3124.631 tons), 25.8% higher than Scheme 1. Scheme 5 also shows significantly higher emissions (2858.299

tons). This underscores the essential role of cooperative mechanisms in low-carbon system dispatch. Scheme 2 exhibits slightly lower emissions (2391.995 tons) than Scheme 1, possibly due to short-term transaction complexity introduced by blockchain. In the long run, however, blockchain is expected to improve market efficiency and support emission reduction. Scheme 3 achieves the lowest emissions (2313.601 tons), though this may reflect over-optimistic scheduling that could pose operational risks in practice. Scheme 1, integrating all mechanisms, strikes a balance in emissions (2483.127 tons), demonstrating the synergistic value of combining cooperative gaming, blockchain, uncertainty management, and Stackelberg gaming.

In conclusion, Scheme 1, which represents the model constructed in this study, is the optimal solution.

6.2. Analysis of Upper-Level VPP Alliance Decision-Making

Based on Figure 6 and Table 4, it can be observed that after Nash bargaining, the final revenue of the VPP alliance increased by 686.048 CNY, with the MGO's revenue rising by 499.495 CNY and the SESO's revenue by 186.553 CNY. This indicates that the symmetric Nash bargaining method can enhance the alliance's overall revenue. Furthermore, the Nash bargaining theory, when applied to the distribution of cooperative surplus within the alliance, adequately addresses fairness and participation incentives among members, thereby promoting equitable and rational distribution within the alliance.

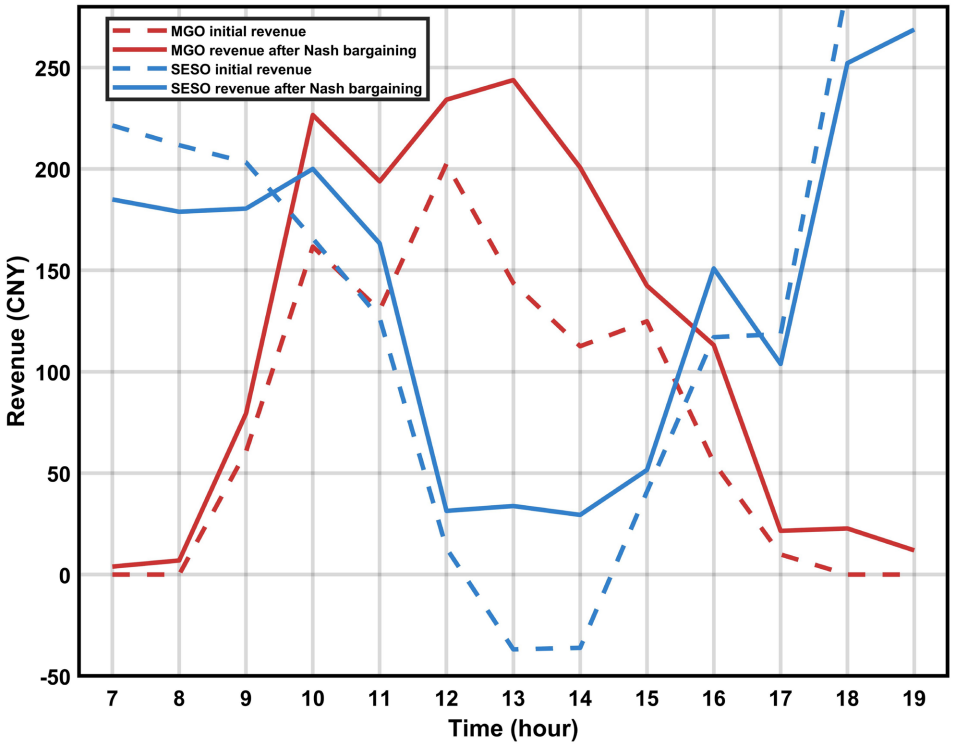

Figure 6. MGO and SESO gains before and after Nash bargaining.

Table 4. VPP alliance benefits and prosumers' electricity utility.

Scheme	VPP revenue/CNY	MGO revenue/CNY	SESO revenue/CNY
Before Nash bargaining	2752.126	1001.386	1750.74
after Nash bargaining	3438.174	1500.881	1937.293

From **Figure 7**, it can be observed that during 7:00-9:00 and 17:00-19:00, the internal electricity purchase price does not exceed 0.8 CNY/kWh, while during 10:00-16:00, it remains below 1.2 CNY/kWh. This reflects the protection of prosumers' welfare in electricity procurement under ToU pricing constraints. During 12:00-15:00, when the system's total electricity sales volume is lower than the purchase volume, the VPP alliance increases the internal selling price to encourage electricity consumption, aiming to incentivize more prosumers to sell electricity. Conversely, during 10:00-12:00 and 15:00-18:00, when electricity purchases are lower than sales, the VPP alliance reduces the internal purchase price to motivate prosumers to consume and purchase more electricity during these periods. By implementing such internal pricing strategies, the VPP alliance guides prosumers toward rational electricity consumption, thereby enhancing system operational efficiency and the local PV consumption rate.

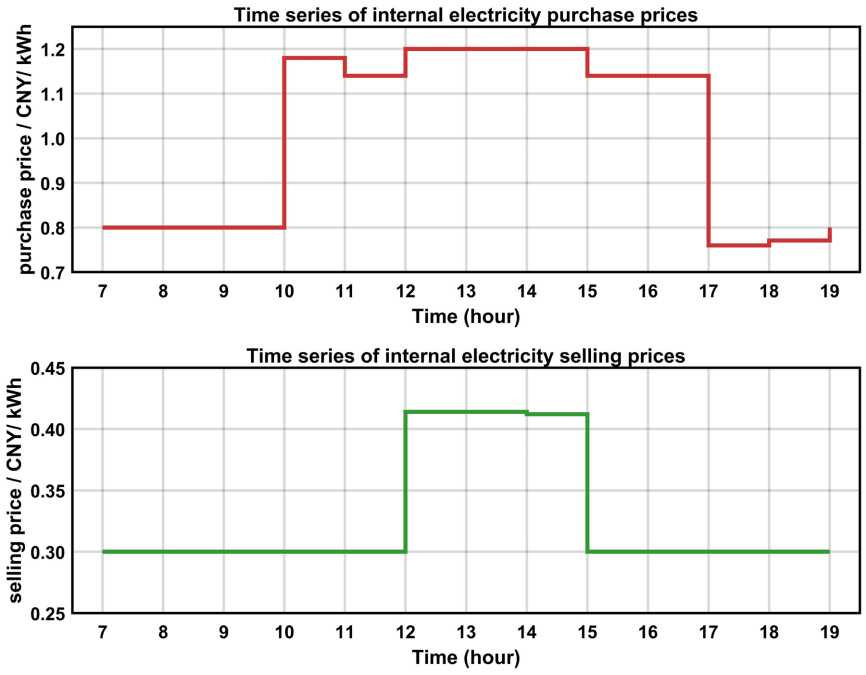

Figure 7. Internal prices changes.

Figure 8 illustrates the variation of the internal interactive electricity price over time when the VPP alliance engages in cooperative gaming, *i.e.*, during electricity interactions between the MGO and SESO. By analyzing the optimized electricity consumption patterns of prosumers, it can be concluded that the system operates

in a net electricity selling mode during 12:00-14:00, and in a net purchasing mode during all other periods. During 7:00-12:00, the MGO purchases electricity from the SESO. Constrained by ToU pricing and the low overall system load during this period, the SESO sets a lower internal interactive price to encourage the MGO to increase its electricity purchases. Compared to purchasing electricity directly from the main grid at real-time prices, this approach reduces the MGO's procurement costs while ensuring revenue for the SESO. During 12:00-14:00, the MGO sells electricity to the SESO, and the internal interactive price decreases as the sales volume increases. Compared to selling electricity directly to the main grid at feed-in tariffs, this strategy increases the MGO's revenue while safeguarding the SESO's earnings. During 15:00-19:00, when the system load peaks and gradually declines, the internal interactive price reaches it's maximum to guide reasonable electricity consumption behavior and optimize power dispatch. As the load decreases, the price correspondingly drops, following a logic consistent with the low-load period in the early morning. Similarly, this approach reduces the MGO's procurement costs while ensuring the SESO's revenue. Furthermore, by combining Table 3 and Figure 8, it is evident that the MGO possesses stronger bargaining power compared to the SESO.

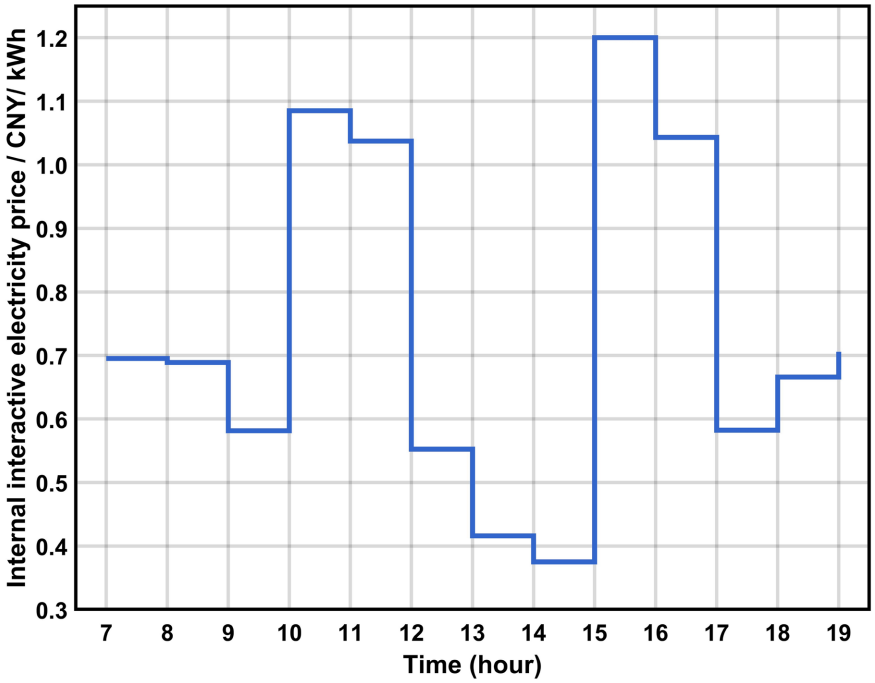

Figure 8. Internal interactive electricity price within VPP.

6.3. Uncertainty Analysis

A comparison of VPP alliance revenue and prosumer utility under different confidence levels is shown in the figure below.

As clearly shown in Figure 9, as the confidence level increases, the boundary of the probability distribution fuzzy set for power generation expands, leading to a

decrease in both the revenue of the VPP alliance and the electricity utility of prosumers. This occurs because the VPP aims to mitigate uncertainty risks in operational decision-making, resulting in more robust decisions at the expense of economic benefits. Within the VPP alliance, as the confidence level decreases, the revenue growth of the MGO is significantly higher than that of the SESO. This is attributed to the MGO's more critical role in this electricity trading model, where it acts as an energy hub by interacting with both prosumers and the SESO, thereby possessing stronger bargaining power. This uncertainty model is designed to ensure that the VPP alliance fully assesses potential risks during decision-making, balancing the relationship between risk and revenue through the constructed model, thereby enhancing the robustness and resilience of system operation.

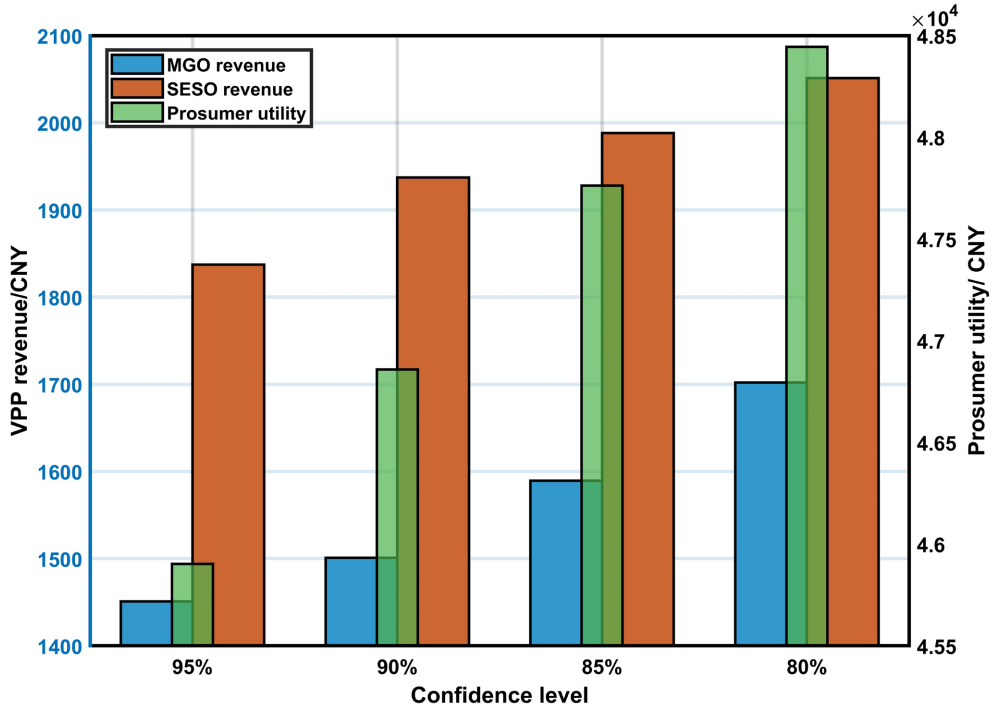

Figure 9. VPP coalition revenues and utility of prosumers at different confidence levels.

6.4. Algorithm Convergence Validation

To verify the computational reliability of the proposed hybrid game model, the convergence performance of the ADMM algorithm is evaluated.

As shown in Figure 10, the primal residual $\left\|r^k\right\|_2$ and dual residual $\left\|s^k\right\|_2$ are tracked across the iterations. Both residuals exhibit a rapid descending trend during the initial iterations and gradually stabilize. After approximately 70 iterations, both the primal and dual residuals drop below the predefined convergence tolerance of 10^{-3}. This quantitative indicator demonstrates that the internal pricing and energy trading strategies between the VPP alliance and the prosumer cluster have reached a stable equilibrium, confirming the algorithmic efficiency and solution feasibility of the developed mode.

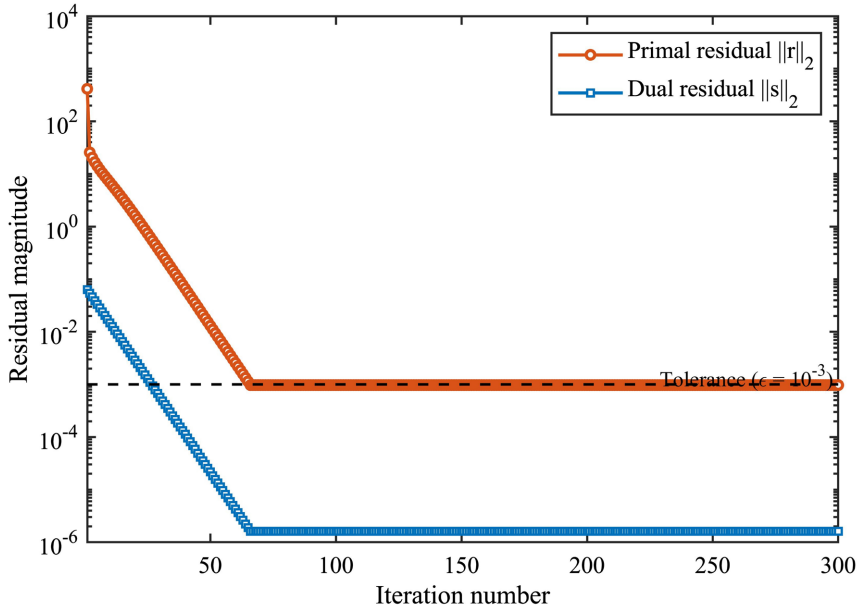

Figure 10. Convergence curves of the ADMM algorithm.

7. Conclusions

Under the "dual carbon" policy framework, this study develops a two-stage bi-level distributed robust optimization model for VPPs under blockchain technology, addressing local consumption of distributed energy, scheduling, and risk management. Key findings are summarized as follows:

1) Synergy between MGO and SESO: Shared energy storage improves local PV consumption, optimizes prosumer behavior, and boosts economic returns for both entities within a VPP alliance. The cooperation also reduces system carbon emissions, enhancing environmental performance alongside operational efficiency and prosumer utility.

2) Blockchain advantages: Distributed ledger and smart contract features increase transparency and fairness, lower transaction costs, and improve system efficiency.

3) Robust uncertainty handling: The Wasserstein-based model strengthens system resilience and supports risk-informed decision-making, balancing economic and reliability objectives.

While the model effectively optimizes upper-level VPP decisions, prosumer-level strategies remain relatively simplistic. Future work will focus on prosumer-centric mechanisms to better align trading and scheduling behaviors, promote fairness, and advance the architecture of distributed energy markets.

Conflicts of Interest

The authors declare no conflicts of interest regarding the publication of this paper.

References

[1] Zhou, W., Zhou, F. and Zhuang, G. (2024) Megacity Pathways in China under the

Dual Carbon Goal: The Case of Shanghai. *Chinese Journal of Population, Resources and Environment*, **22**, 241-249. https://doi.org/10.1016/j.cjpre.2024.09.003

[2] Li, X., Zheng, Z., Luo, B., Shi, D. and Han, X. (2024) The Impact of Electricity Sales Side Reform on Energy Technology Innovation: An Analysis Based on SCP Paradigm. *Energy Economics*, **136**, Article 107763. https://doi.org/10.1016/j.eneco.2024.107763

[3] Beyea, J. (2010) The Smart Electricity Grid and Scientific Research. *Science*, **328**, 979-980. https://doi.org/10.1126/science.1189229

[4] Zare, A., Shafie-Khah, M., Siano, P. and Lazaroiu, G.C. (2026) A Systematic Review of Virtual Power Plant Configurations and Their Interaction with Electricity, Carbon, and Flexibility Markets. *Renewable and Sustainable Energy Reviews*, **226**, Article 116448. https://doi.org/10.1016/j.rser.2025.116448

[5] Li, J., Fang, Z., Wang, Q., Zhang, M., Li, Y. and Zhang, W. (2024) Optimal Operation with Dynamic Partitioning Strategy for Centralized Shared Energy Storage Station with Integration of Large-Scale Renewable Energy. *Journal of Modern Power Systems and Clean Energy*, **12**, 359-370. https://doi.org/10.35833/mpce.2023.000345

[6] Wang, W., Kong, Z., He, Y., Li, C. and Jia, K. (2024) Research on the Collaborative Operation Strategy of Shared Energy Storage and Virtual Power Plant Based on Double Layer Optimization. *Journal of Energy Storage*, **101**, Article 113997. https://doi.org/10.1016/j.est.2024.113997

[7] Lin, M., Liu, J., Tang, Z., Zhou, Y., Jiang, B., Zeng, P., *et al.* (2025) Coordinated DSO-VPP Operation Framework with Energy and Reserve Integrated from Shared Energy Storage: A Mixed Game Method. *Applied Energy*, **379**, Article 125006. https://doi.org/10.1016/j.apenergy.2024.125006

[8] Pan, Y., Ju, L., Yang, S., Guo, X. and Tan, Z. (2024) A Multi-Objective Robust Optimal Dispatch and Cost Allocation Model for Microgrids-Shared Hybrid Energy Storage System Considering Flexible Ramping Capacity. *Applied Energy*, **369**, Article 123565. https://doi.org/10.1016/j.apenergy.2024.123565

[9] Li, J., Xu, Z., Liu, H., Wang, C., Wang, L. and Gu, C. (2023) A Wasserstein Distributionally Robust Planning Model for Renewable Sources and Energy Storage Systems under Multiple Uncertainties. *IEEE Transactions on Sustainable Energy*, **14**, 1346-1356. https://doi.org/10.1109/tste.2022.3173078

[10] Li, W., Dong, F., Ji, Z. and Wang, P. (2025) Internal and External Coordinated Distributionally Robust Bidding Strategy of Virtual Power Plant Operator Participating in Day-Ahead Electricity Spot and Peaking Ancillary Services Markets. *Applied Energy*, **386**, Article 125514. https://doi.org/10.1016/j.apenergy.2025.125514

[11] Liu, H., Qiu, J. and Zhao, J. (2022) A Data-Driven Scheduling Model of Virtual Power Plant Using Wasserstein Distributionally Robust Optimization. *International Journal of Electrical Power & Energy Systems*, **137**, Article 107801. https://doi.org/10.1016/j.ijepes.2021.107801

[12] Ming, Z., Zhang, H., Li, Y. and Liang, Y. (2024) Mixed H_2/H_∞ Control for Nonlinear Closed-Loop Stackelberg Games with Application to Power Systems. *IEEE Transactions on Automation Science and Engineering*, **21**, 69-77. https://doi.org/10.1109/tase.2022.3216733

[13] Chang, W. and Yang, Q. (2025) Game-Theoretic Risk-Averse Day-Ahead Optimal Bidding Strategy of Virtual Power Plant Aggregated with Heterogeneous Distributed Resources. *Energy*, **336**, Article 138087. https://doi.org/10.1016/j.energy.2025.138087

[14] Shang, Y., Li, X., Xu, T. and Cui, L. (2025) Uncertainty-Output Virtual Power Plant Participates in Multi-Electricity Market Considering the Improved Shapley Value

Distribution Method. *International Journal of Electrical Power & Energy Systems*, **165**, Article 110462. https://doi.org/10.1016/j.ijepes.2025.110462

[15] Li, N., Gao, Y. and Yin, Y. (2025) Joint Chance-Constrained Real-Time Pricing for Smart Grid with Multi-Energy Generation: A Stochastic Convex Hull-Based Approach. *Sustainable Energy, Grids and Networks*, **43**, Article 101809. https://doi.org/10.1016/j.segan.2025.101809

[16] Li, N. and Gao, Y. (2023) Real-Time Pricing Based on Convex Hull Method for Smart Grid with Multiple Generating Units. *Energy*, **285**, Article 129543. https://doi.org/10.1016/j.energy.2023.129543

[17] Dai, Y., Gao, Y., Gao, H. and Zhu, H. (2017) Real-Time Pricing Scheme Based on Stackelberg Game in Smart Grid with Multiple Power Retailers. *Neurocomputing*, **260**, 149-156. https://doi.org/10.1016/j.neucom.2017.04.027

[18] Hosseini Dehshiri, S.J., Amiri, M., Mostafaeipour, A. and Le, T. (2024) Integrating Blockchain and Strategic Alliance in Renewable Energy Supply Chain toward Sustainability: A Comparative Decision Framework under Uncertainty. *Energy*, **304**, Article 132136. https://doi.org/10.1016/j.energy.2024.132136

[19] Leng, J. and Cheng, Y. (2025) Investing in a Zero-Carbon Future: Game-Theoretic Strategies for Clean Energy and Blockchain in Commercial Buildings. *Energy and Buildings*, **347**, Article 116323. https://doi.org/10.1016/j.enbuild.2025.116323

[20] Ke, Y., Chen, Z., Feng, C., Xie, M., Zhu, K. and Su, J. (2025) A Blockchain-Based P2P Regional Energy Trading and Credit Mechanism. *Energy Conversion and Management: X*, **28**, Article 101193. https://doi.org/10.1016/j.ecmx.2025.101193

[21] Sindi, H.F., Morgan, M., Shaaban, M., Zeineldin, H.H. and Lasheen, A. (2024) Blockchain-Based Energy Trading in Droop-Based Hybrid Microgrids. *Ain Shams Engineering Journal*, **15**, Article 102848. https://doi.org/10.1016/j.asej.2024.102848

[22] Chen, Y., Li, Y., Chen, Q., Wang, X., Li, T. and Tan, C. (2023) Energy Trading Scheme Based on Consortium Blockchain and Game Theory. *Computer Standards & Interfaces*, **84**, Article 103699. https://doi.org/10.1016/j.csi.2022.103699

[23] Shen, W., Ding, H., Zeng, M. and Zhang, X. (2025) Optimal Bidding Strategy for Integrated Energy System Participating in Spot Power Market: A Wasserstein Metric Based DRO Method. *Energy*, **327**, Article 136402. https://doi.org/10.1016/j.energy.2025.136402

[24] Blanchet, J. and Si, N. (2019) Optimal Uncertainty Size in Distributionally Robust Inverse Covariance Estimation. *Operations Research Letters*, **47**, 618-621. https://doi.org/10.1016/j.orl.2019.10.005

[25] Mohajerin Esfahani, P. and Kuhn, D. (2017) Data-Driven Distributionally Robust Optimization Using the Wasserstein Metric: Performance Guarantees and Tractable Reformulations. *Mathematical Programming*, **171**, 115-166. https://doi.org/10.1007/s10107-017-1172-1

[26] Huang, H., Miao, P., Wei, Q. and Geng, Y. (2026) Bilevel Optimization in Smart Grid Operations: A Review of Real-Time Electricity Pricing Strategies and Future Directions. *Electric Power Systems Research*, **251**, Article 112253. https://doi.org/10.1016/j.epsr.2025.112253

[27] Zheng, X., Li, Q., Bai, C., Nie, Y. and Huang, C. (2022) Energy Trading Management Based on Stackelberg Game Theory to Increase Independence of Microgrids. *Energy Reports*, **8**, 771-779. https://doi.org/10.1016/j.egyr.2022.10.168

[28] Hu, Z., Zhu, Z., Wei, X., Chan, K.W. and Bu, S. (2025) Mixed Strategy Nash Equilibrium Analysis in Real-Time Pricing and Demand Response for Future Smart Retail

Market. *Applied Energy*, **391**, Article 125815.
https://doi.org/10.1016/j.apenergy.2025.125815

[29] Samadi, P., Mohsenian-Rad, A., Schober, R., Wong, V.W.S. and Jatskevich, J. (2010) Optimal Real-Time Pricing Algorithm Based on Utility Maximization for Smart Grid. 2010 *First IEEE International Conference on Smart Grid Communications*, Gaithersburg, 4-6 October 2010, 415-420.
https://doi.org/10.1109/smartgrid.2010.5622077

[30] Habib, S., El-Ferik, S., Gulzar, M.M., Chauhdary, S.T., Ahmed, E.M. and Alnuman, H. (2025) A Tri-Level Hierarchical Optimization Framework for Smart Homes, Microgrids, and Distribution Networks with Hydrogen Integration Using a Distributed ADMM Approach. *Applied Energy*, **400**, Article 126577.
https://doi.org/10.1016/j.apenergy.2025.126577

[31] Cao, J., Yang, D. and Dehghanian, P. (2024) Cooperative Operation for Multiple Virtual Power Plants Considering Energy-Carbon Trading: A Nash Bargaining Model. *Energy*, **307**, Article 132813. https://doi.org/10.1016/j.energy.2024.132813

Appendix A

By observing Equations (23)-(27), it is evident that in the follower model, since the electricity consumption x_n^i is naturally greater than or equal to 0, the DRO model of the prosumer's electricity utility is a continuous and strictly concave function with respect to x_n^i. Setting the first-order derivative of Equation (27) to zero, we obtain the maximum point of the function as:

$$\begin{cases} x_n^{i*} = \sqrt{\dfrac{k_{n,blo}^{i^2}}{p_b^{i^2}} - 1} & n \in \chi_b \\ x_n^{i*} = \sqrt{\dfrac{k_{n,blo}^{i^2}}{p_s^{i^2}} - 1} & n \in \chi_s \end{cases} \tag{A.1}$$

Subsequently, substituting x_n^{i*} back into Equations (23) and (25), the leader model can be derived as:

$$\begin{cases} \max\limits_{p_n^i, \lambda_1^i} \left(\sum\limits_{n \in \chi_b} \left(\sqrt{\dfrac{k_{n,blo}^{i^2}}{p_b^{i^2}} - 1} - \dfrac{1}{|J|} \sum\limits_{j \in J} Q_{n,j}^{i,re} \right) p_b^i - \sum\limits_{n \in \chi_s} \left(\dfrac{1}{|J|} \sum\limits_{j \in J} Q_{n,j}^{i,re} - \sqrt{\dfrac{k_{n,blo}^{i^2}}{p_s^{i^2}} - 1} \right) p_s^i + p_{peek} P_{ch}^i - P_{ch}^i \eta_{om} - \lambda_1^i \varepsilon_{PV} \right) & \overline{T}_s^{i,re} > \overline{T}_b^{i,re}, \lambda_1^i \geq p_b^i \\ \max\limits_{p_n^i, \lambda_1^i} \left(\sum\limits_{n \in \chi_b} \left(\sqrt{\dfrac{k_{n,blo}^{i^2}}{p_b^{i^2}} - 1} - \dfrac{1}{|J|} \sum\limits_{j \in J} Q_{n,j}^{i,re} \right) p_b^i - \sum\limits_{n \in \chi_s} \left(\dfrac{1}{|J|} \sum\limits_{j \in J} Q_{n,j}^{i,re} - \sqrt{\dfrac{k_{n,blo}^{i^2}}{p_s^{i^2}} - 1} \right) p_s^i - p_{val} P_{dis}^i - P_{dis}^i \eta_{om} - \lambda_1^i \varepsilon_{PV} \right) & \overline{T}_s^{i,re} \leq \overline{T}_b^{i,re}, \lambda_1^i \geq p_b^i \end{cases} \tag{A.2}$$

From the above equation, it is evident that the leader model is a continuously differentiable function with respect to $\left(p_b^i, p_s^i\right)$, meaning there exists $\left(p_b^{i*}, p_s^{i*}\right)$ that optimizes the leader model. Thus, the existence of the Stackelberg game equilibrium solution is proven.

Next, the Hessian matrix of Equation (A.2) with respect to p_b^i and p_s^i can be derived as:

$$\begin{bmatrix} \sum\limits_{n \in \chi_b} -\left(k_{n,blo}^{i^2} - p_b^{i^2}\right)^{-\frac{1}{2}} \left(1 + p_b^{i^2} \left(k_{n,blo}^{i^2} - p_b^{i^2}\right)^{-1}\right) & 0 \\ 0 & \sum\limits_{n \in \chi_s} -\left(k_{n,blo}^{i^2} - p_s^{i^2}\right)^{-\frac{1}{2}} \left(1 + p_s^{i^2} \left(k_{n,blo}^{i^2} - p_s^{i^2}\right)^{-1}\right) \end{bmatrix} \tag{A.3}$$

From the above matrix, it is clear that according to Equation (27), since $k_n^i \geq p_n^i$, the Hessian matrix of the leader model with respect to p_b^i and p_s^i is negative definite. Therefore, the leader model is a continuously differentiable strictly concave function, meaning there exists a unique optimal point $\left(p_b^{i*}, p_s^{i*}\right)$ that achieves the optimal value for the model.

Hence, the uniqueness of the Stackelberg game equilibrium solution is proven.

Appendix B

To prove that the cooperative game between the MGO and SESO is superadditive, it suffices to show that for any time period, $R_{VPP}^{i}\left(\lambda_1^i, p_n^i\right) - R_{SESO,0}^{i} - R_{MGO,0}^{i} \geq 0$. When no alliance is formed, the revenues of the SESO and MGO can be expressed respectively as:

$$R_{MGO,0}^{i} = \begin{cases} \overline{T}_b^{i,re} p_b^i - \overline{T}_s^{i,re} p_s^i + p_{ol}\left(\overline{T}_s^{i,re} - \overline{T}_b^{i,re}\right) - \lambda_1^i \varepsilon_{PV}, & \overline{T}_s^{i,re} > \overline{T}_b^{i,re}, \lambda_1^i \geq p_b^i \\ \overline{T}_b^{i,re} p_b^i - \overline{T}_s^{i,re} p_s^i + p_{bs,r}\left(\overline{T}_s^{i,re} - \overline{T}_b^{i,re}\right) - \lambda_1^i \varepsilon_{PV}, & \overline{T}_s^{i,re} \leq \overline{T}_b^{i,re}, \lambda_1^i \geq p_b^i \end{cases} \tag{B.1}$$

where p_{ol} and $p_{bs,r}$ represent the photovoltaic feed-in tariff and the commercial real-time electricity price, respectively.

$$R_{SESO,0}^{i} = \left(p_{peek}\eta_{dis}\eta_{ch} - p_{val}/\eta_{dis}\eta_{ch}\right)\left(\overline{T}_b^{i,re} - \overline{T}_s^{i,re}\right) - \eta_{om}\left(\overline{T}_b^{i,re} + \overline{T}_s^{i,re}\right) \tag{B.2}$$

Next, we obtain:

1) If $\overline{T}_s^{i,re} > \overline{T}_b^{i,re}$:

$$\begin{aligned} & R_{VPP}^{i}\left(\lambda_1^i, p_n^i\right) - R_{SESO,0}^{i} - R_{MGO,0}^{i} \\ &= \overline{T}_b^{i,re} p_b^i - \overline{T}_s^{i,re} p_s^i + \eta_{dis}\eta_{ch} p_{peek} P_{ch}^i - P_{ch}^i \eta_{om} - \lambda_1^i \varepsilon_{PV} \\ &\quad - \left(p_{peek}\eta_{dis}\eta_{ch} - p_{val}/\eta_{dis}\eta_{ch}\right)\left(\overline{T}_b^{i,re} - \overline{T}_s^{i,re}\right) + \eta_{om}\left(\overline{T}_b^{i,re} + \overline{T}_s^{i,re}\right) \\ &\quad - \overline{T}_b^{i,re} p_b^i + \overline{T}_s^{i,re} p_s^i - p_{ol}\left(\overline{T}_s^{i,re} - \overline{T}_b^{i,re}\right) + \lambda_1^i \varepsilon_{PV} \end{aligned} \tag{B.3}$$

2) If $\overline{T}_s^{i,re} \leq \overline{T}_b^{i,re}$:

$$\begin{aligned} & R_{VPP}^{i}\left(\lambda_1^i, p_n^i\right) - R_{SESO,0}^{i} - R_{MGO,0}^{i} \\ &= \overline{T}_b^{i,re} p_b^i - \overline{T}_s^{i,re} p_s^i - p_{val}/\eta_{dis}\eta_{ch} P_{dis}^i - P_{dis}^i \eta_{om} - \lambda_1^i \varepsilon_{PV} \\ &\quad - \left(p_{peek}\eta_{dis}\eta_{ch} - p_{val}/\eta_{dis}\eta_{ch}\right)\left(\overline{T}_b^{i,re} - \overline{T}_s^{i,re}\right) + \eta_{om}\left(\overline{T}_b^{i,re} + \overline{T}_s^{i,re}\right) \\ &\quad - \overline{T}_b^{i,re} p_b^i + \overline{T}_s^{i,re} p_s^i - p_{bs,r}\left(\overline{T}_s^{i,re} - \overline{T}_b^{i,re}\right) + \lambda_1^i \varepsilon_{PV} \end{aligned} \tag{B.4}$$

Moreover, since during overall system electricity sales $P_{ch}^i = \overline{T}_s^{i,re} - \overline{T}_b^{i,re}$, and during overall electricity purchases $P_{dis}^i = \overline{T}_b^{i,re} - \overline{T}_s^{i,re}$. Simplifying Equations (B.3) and (B.4) yields:

1) If $\overline{T}_s^{i,re} > \overline{T}_b^{i,re}$:

$$\left(2\eta_{dis}\eta_{ch} p_{peek} - p_{val}/\eta_{dis}\eta_{ch} - p_{ol}\right)\left(\overline{T}_s^{i,re} - \overline{T}_b^{i,re}\right) + 2\overline{T}_b^{i,re}\eta_{om} \tag{B.5}$$

2) If $\overline{T}_s^{i,re} \leq \overline{T}_b^{i,re}$:

$$\left(p_{bs,r} - p_{peek}\eta_{dis}\eta_{ch}\right)\left(\overline{T}_b^{i,re} - \overline{T}_s^{i,re}\right) + 2\overline{T}_s^{i,re}\eta_{om} \tag{B.6}$$

From Equation (B.5), it can be observed that since $\overline{T}_s^{i,re} > \overline{T}_b^{i,re}$, and $2\eta_{dis}\eta_{ch} p_{peek} - p_{val}/\eta_{dis}\eta_{ch} - p_{ol} > 0$, Equation (B.5) is greater than or equal to 0. In Equation (B.6), since $\overline{T}_s^{i,re} \leq \overline{T}_b^{i,re}$, and $p_{bs,nr} - p_{peek}\eta_{dis}\eta_{ch} > 0$, Equation (B.6) is greater than or equal to 0.

In conclusion, the superadditivity between the MGO and SESO—*i.e.*, Equation (31)—is thereby proved.